



Total electron content (TEC) variability at Los Alamos, New Mexico: A comparative study:

2. Comparisons with other TEC sources

Zhen Huang¹ and Robert Roussel-Dupré¹

Received 25 October 2004; revised 3 May 2006; accepted 20 July 2006; published 9 December 2006.

[1] In this study, the Fast On-Orbit Recording of Transient Events (FORTE) derived TEC variabilities on a diurnal cycle, seasonal cycle, 11-year solar cycle, and 27-day solar cycle are compared with the TEC estimates from the Los Alamos ionospheric transfer function implemented with the International Reference Ionosphere model, the GPS-derived TEC maps from NOAA, the GPS measurements made at Los Alamos, and the ionosonde critical frequency data at the closest station, Boulder, Colorado. The results show good agreement on average (monthly, annual, or multiyear means) in TEC variability at Los Alamos between the various data sources with relative RMS errors of about 5–10%. The results also show RMS errors larger than 30% for point-to-point comparisons, with the most significant errors found during high solar activity years, during summer seasons, and during strong geomagnetic storm conditions. This comparative study suggests that the FORTE-derived TECs combined with other TEC sources can help to better understand the TEC variability at Los Alamos in providing more accurate time-dependent site TECs than those derived from a single source or extrapolated from global model predictions.

Citation: Huang, Z., and R. Roussel-Dupré (2006), Total electron content (TEC) variability at Los Alamos, New Mexico: A comparative study: 2. Comparisons with other TEC sources, *Radio Sci.*, 41, RS6004, doi:10.1029/2004RS003203.

1. Introduction

[2] Different methods have been applied to characterize ionospheric total electron content (TEC). One of the most common comparative studies has been made between direct ionospheric measurements and various ionospheric model predictions. *Brown et al.* [1991] used the TEC data from a wide range of latitudes and longitudes for a complete range of solar activity to evaluate the performance of six ionospheric models as predictors of TEC. These ionospheric models include (1) the International Reference Ionosphere (IRI), (2) the Bent model, (3) the Ionospheric Conductivity and Electron Density (ICED) model, (4) the Penn State model, (5) the Fully Analytic Ionospheric Model (FAIM), and (6) the Damen-Hartranft model. They made extensive comparisons between monthly mean TEC at all local

times and model TEC obtained by integrating electron density profiles produced by the six models. They have found that the models can generally describe the diurnal variations of the ionospheric TEC but can exhibit large discrepancies from direct ionospheric measurements. They suggested that such discrepancies may be caused by inaccurate representation of the topside scale height. Comparative studies between the TECs from Ocean Topography Experiment (TOPEX) measurements for 1992–1997 and the Bent and IRI model predicted TEC values indicated a model underestimation bias of 1.7 (IRI) and 2.2 (Bent) TECU (1 TECU = 10^{16} el/m²) on average at high latitudes which reflect the absence of auroral contributions in the empirical models. The bias at midlatitudes on the other hand is very small [*Codrescu et al.*, 2001]. A comparison between the Global Positioning Satellite (GPS) derived TECs and the IRI model predictions at midlatitude (Matera, 40.6°N, 24.4°E) during the low solar activity years (1996–1997) indicates an overprediction of GPS TECs with differences of as high as 50% (or 2–4 TECU) of the diurnal TEC depending on season (maximum in winter and autumn, minimum in summer) and time of day (large at nighttime and small at daytime) [*Ephishov et al.*, 2000]. *Sethi et al.* [2001] use

¹Atmospheric, Environmental and Climatic Dynamics Group, Earth and Environmental Sciences Division, Los Alamos National Laboratory, Los Alamos, New Mexico, USA.

the incoherent scatter radar data from Arecibo (18.4°N, 66.7°W) to evaluate the performance of IRI. They found that the IRI model overestimates the observed TEC for all local times during equinox and summer but shows good agreement in winter.

[3] Many comparative studies have been conducted between GPS TEC measurements and other direct measurements. *Conkright et al.* [1997] compared TECs at Boulder, Colorado (40.0°N, 105.2°W), derived from observations of GPS and those obtained using the Faraday rotations from the Geostationary Operational Environmental Satellites (GOES) 2 geosynchronous satellite. They found relatively good agreement for diurnal variations and general agreement in seasonal cycle with sufficient smoothing over space and time. Furthermore, TECs derived from different GPS receivers at two nearby stations spaced about 50 km apart are quite consistent with RMS differences in TEC of 0.3–1.0 TECU. They found that the nighttime GPS TECs are higher than those from GOES 2. *Ho et al.* [1997] compared the GPS-derived TECs with ionospheric measurements from the TOPEX altimeter. Their results indicated that the difference in the two TEC measurements is less than 1.5 TECU within a 1500 km range from a reference GPS station and that the RMS gradually increases with increasing distance from the station. The differences become relatively large during ionospheric disturbed periods. A similar comparative study using a restricted (within 5° of the zenith angle) TOPEX altimeter data set found that the GPS TECs were in agreement with the TOPEX measured TECs at the 2–3 TECU difference level in the midlatitudes (30°–55°) relative to a typical daily maximum TEC of ~80 TECU [*Mannucci et al.*, 1994].

[4] An International GPS Service (IGS) report documented in details on the comparisons between the TOPEX TEC and the GPS TECs from the five IGS Ionosphere Associate Analysis Centers (IAACs): Center for Orbit Determination in Europe (CODE), Astronomical Institute, University of Berne, Switzerland; European Space Operations Center (ESOC) of ESA, Darmstadt, Germany; Jet Propulsion Laboratory (JPL), Pasadena, California, United States; Natural Resources Canada (NRC/EMR), Ottawa, Ontario, Canada; and Technical University of Catalonia (UPC), Barcelona, Spain (International GPS Service, Performance of IGS ionosphere TEC maps, IGS Ionosphere Working Group report, 16 pp., Technical University of Catalonia, Barcelona, Spain, 2003, available at http://maite152.upc.es/~ionex3/doc/IGS_IONO_report_April2003_7.pdf.) The TOPEX TEC and the GPS TEC are compared for validations that are required to facilitate GPS TEC mappings to an official operation status. The different IAAC TEC maps have been computed with different approaches but with a common formal resolution of 2 hours in UT and 5° and

2.5° in longitude and latitude using the 2,500,000 TOPEX observations during the period from 15 December 2002 to 15 March 2003. It shows that the GPS TECs have a mostly positive bias (4 out of 5) ranging from 0.8 to 4.8 TECU and one negative bias of –1.0 TECU. The report noted that their comparison provides a lower boundary for the GPS TEC performance.

[5] In a companion paper [*Huang and Roussel-Dupré*, 2005], data collected from the Fast On-Orbit Recording of Transient Events (FORTE) satellite received Los Alamos Portable Pulsar (LAPP) signals during 1997–2002 are used to derive TECs at Los Alamos, New Mexico. The FORTE satellite was launched on 29 August 1997. It is in a circular, 800-km-altitude orbit inclined 70° from the Earth's equator. The FORTE radio payload is a set of tunable wideband radio receivers (26–100 MHz) to provide data on the propagation of broadband radio signals through the ionosphere. Such data can be used to study ionospheric properties, such as changes in TEC, which produces variations in the amount of dispersion of a transient broadband RF signal [*Jacobson et al.*, 1999]. The LAPP is an electromagnetic pulse generator coupled to a 30 m dish/antenna, located at Los Alamos, New Mexico (35.872°N, 106.327°W, elevation 2274.08 m). Readers can find detailed FORTE-LAPP data descriptions in the work by *Huang and Roussel-Dupré* [2005].

[6] We have presented the variabilities of the FORTE-derived TECs at Los Alamos for diurnal, seasonal, interannual, and 27-day solar cycle in the companion paper [*Huang and Roussel-Dupré*, 2005]. In that paper, we have analyzed the effects of several technical aspects on deriving and converting TEC, including slant-to-vertical TEC conversion, quartic effects on transionospheric signals, and the thin shell assumption. We also examined geomagnetic storm effects on the TEC variance superimposed on the averaged TEC values. We concluded that those effects need to be particularly considered under certain circumstances but they do not affect the results significantly in general. By comparing FORTE-derived TECs to other TEC sources, our main objectives of this paper are (1) to validate the FORTE-derived TECs, (2) to explore if there are any significant discrepancies, and (3) to indicate specific time/conditions for these discrepancies.

2. Comparisons With IRI-ITF Model Predictions

[7] In this section, we present results on the TEC variabilities at Los Alamos simulated by the International Ionospheric Reference (IRI) model for the period of time from 1997 to 2002. Slant TECs are computed from the IRI model coupled with the ionospheric transfer function

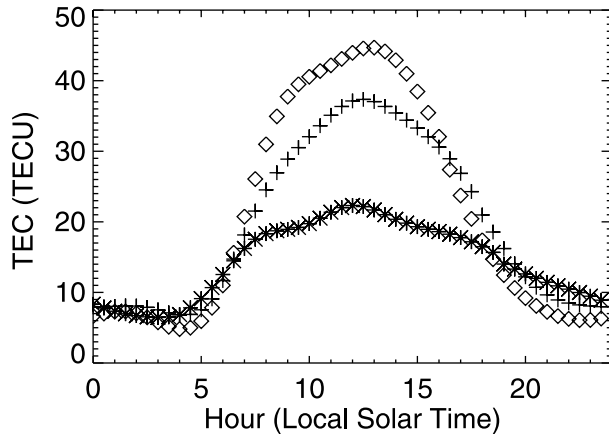


Figure 1. IRI model-predicted TEC diurnal cycle averaged over 1997–2002 for March (pluses), July (asterisks), and November (diamonds).

(ITF) and are compared with the corresponding FORTE-derived TECs on the diurnal, seasonal, and interannual timescales, as well as 27-day solar cycle. RMS error analyses are conducted to examine the differences in the comparisons.

2.1. IRI Model and ITF Model Description

[8] The IRI model [Bilitza, 2001] is a global empirical model, which specifies the averages of the electron density, electron temperature, ion temperature, and ion composition from 80 to 2000 km. The IRI also predicts vertical TEC averages for magnetically quiet conditions. As an empirical model, the IRI is naturally only as good as the available observations. The data sources used in the IRI model include ionosonde, incoherent scatter, rocket, and satellite measurements. The IRI model predicts TEC on the basis of the F_2 region critical frequency and height. Since the F_2 region critical frequency and height are from real-time spatial maps of ground-based ionosonde measurements mostly located in the midlatitudes, the IRI does an excellent job of specifying the ionospheric TEC climatology at midlatitudes. The latest IRI model, IRI2001, is used to generate TEC variabilities at Los Alamos for 1997–2002 on diurnal, seasonal, interannual timescales, and 27-day solar cycle.

[9] The ionospheric transfer function (ITF) has been developed to perform integrals along the slant path from a specified transmitter to a specified receiver given the electron density and geomagnetic field vector for the radio frequencies of interest much larger than the plasma frequency [Roussel-Dupré et al., 2001]. The ITF takes into consideration the phase change corrections along the slant path introduced by the ionosphere including the integrated electronic density effect, higher-order integral

moments of electronic density, and refractive bending. The ITF function is used to couple with the IRI model in estimating slant TECs along a raypath through the ionosphere from the LAPP transmitter to FORTE satellite receiver for the given time and date of a LAPP event.

2.2. IRI Model-Predicted TEC Analysis

[10] The IRI model was used to simulate vertical TEC at Los Alamos for the period of 1997–2002 at half an hour temporal resolution. For the FORTE-LAPP data used in this study, the altitude of the FORTE satellite varies from 798.35 to 843.84 km. In predicting IRI TEC, we set the model altitude to an average of 820 km. Figure 1 gives the 1997–2002 6-year mean TEC diurnal variations for March (pluses sign), July (asterisks), and November (diamonds). We can see that the IRI model-simulated TEC displays a diurnal cycle with peaks at 1200–1300 LT and lows at around 0400 LT. The magnitude of the diurnal cycle changes from a minimum of 5 TECU to a maximum of 45 TECU, a factor of ~ 9 . The diurnal peak varies with season largely from about 22 TECU in July to 37–45 TECU in March and November, a factor of 1.7–2.1. The diurnal low remains relatively stable in absolute TEC value, changing from 5 TECU in November to about 7 TECU in March and July, a factor of 1.4.

[11] The IRI model-simulated TEC shows a daytime seasonal cycle with semiannual peaks in March and October to November, a major low in June to July, and a secondary low in December–January (Figure 2). The nighttime seasonal TEC cycle does not appear to be semiannual. As a result, we can see that the daytime-nighttime difference in TEC is much smaller during the warm season than that during the cold season. The amplitude of daytime-averaged seasonal TEC varies

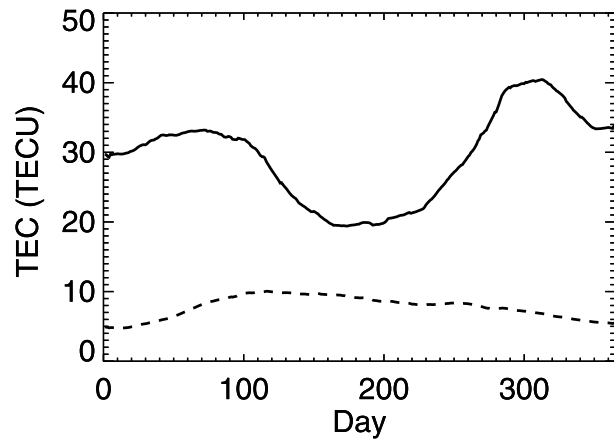


Figure 2. IRI model-predicted TEC 1997–2002 mean seasonal cycle for daytime (0800–1700 LT, solid line) and nighttime (1600–0500 LT, dashed line).

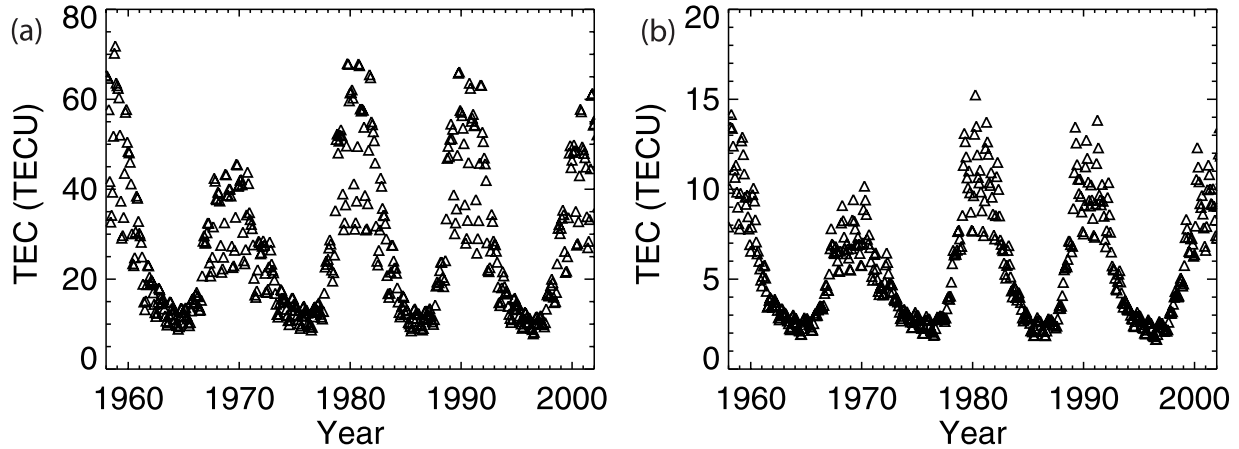


Figure 3. IRI model-predicted TEC 1958–2002 interannual variations for (a) 1200–1400 LT and (b) 0200–0400 LT.

from 20 to 40 TECU, a factor of 2. The nighttime-averaged seasonal TEC varies from the lowest values of about 5 TECU in January to the highest values up to 10 TECU in April to May, also a factor of 2.

[12] Figures 3a and 3b show the IRI-simulated monthly mean TEC variations at Los Alamos from 1958 to 2002 averaged over local solar time from noon to 2 p.m. and from 0200 to 0400 LT, respectively. The 11-year solar cycle is clearly reflected in the TEC interannual variations for both daytime and nighttime. We can see that TEC peaks at solar activity peak years (1958–1959, 1968–1969, 1980–1981, 1990–1991, and 2000–2001) and reaches its lowest phase at the 11-year solar cycle minimum years (1964–1965, 1976–1977, 1985–1986,

and 1996–1997). During daytime the lowest TEC of as low as 7 TECU happened at the 11-year solar cycle minimum while the TECs reached as high as 70 TECU at 11-year solar cycle maximum, a factor of ~ 10 . During nighttime TEC changes from 2 TECU at solar minimum to 14 TECU at solar maximum, a factor of ~ 7 .

[13] It can be also seen from Figure 3 that the amplitude of the TEC seasonal variations increases significantly at high solar activity years compared to that at low solar activity years for both daytime and nighttime. During daytime, the magnitude of the seasonal TEC variations increases from about 5 TECU at low solar activity years to over 40 TECU at high solar activity years. During nighttime, the magnitude is about 1 TECU

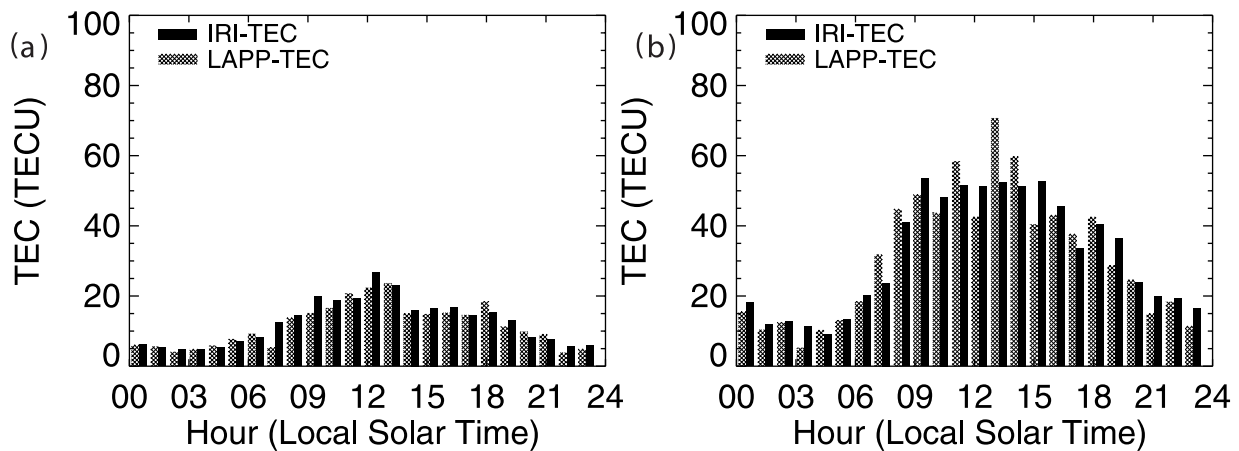


Figure 4. Slant TEC diurnal cycle comparisons between 1997–1998 FORTE-derived and IRI-ITF model-predicted annual mean for (a) slant distance range from 800 to 1000 km and (b) slant distance from 2000 to 2500 km.

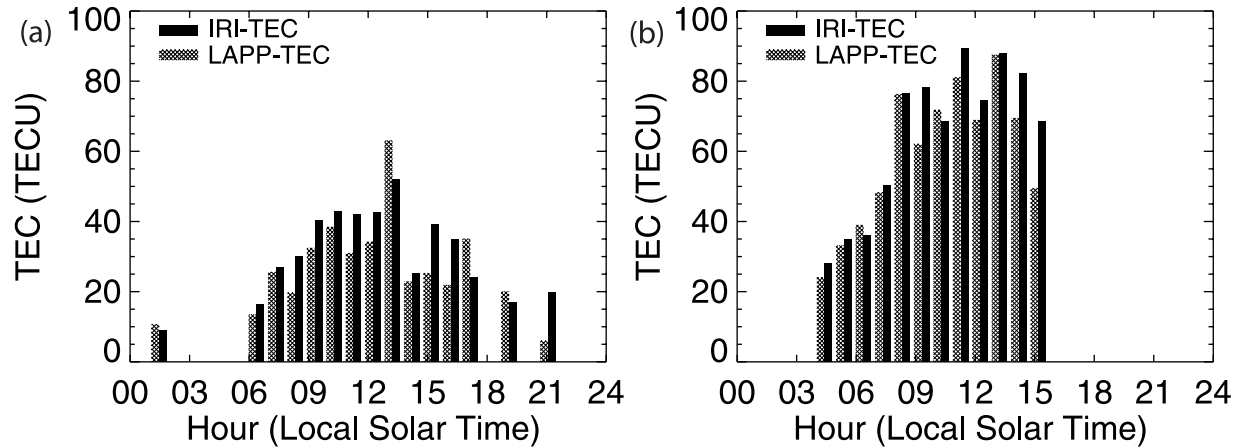


Figure 5. Same as Figure 4 but for 1999–2002.

for low solar activity years and reaches as high as 7 TECU for high solar activity years. Nevertheless, the relative changes in the amplitude of the TEC seasonal variations are always about a factor of 2. Furthermore, during the transition years from high to low solar activity or vice versa, the rapid changes in TEC due to changes in solar activity over the 11-year cycle dominate the TEC seasonal variations resulting in a very weak seasonal cycle.

2.3. FORTE-Derived and IRI-Predicted TEC Comparisons

[14] In this section, the coupled IRI-ITF model was used to predict slant TECs for the LAPP events given the raypath from the FORTE satellite and LAPP transmitter, the date and time, and solar (daily sunspot numbers) and

geomagnetic conditions. The results of the IRI-ITF model-predicted slant TECs were compared with the FORTE-derived slant TECs on different timescales.

2.3.1. Comparisons on Average

[15] Visually, our FORTE-derived slant TEC results show good agreement on average in TEC variabilities on diurnal, seasonal, and interannual timescales with the IRI-ITF model-predicted slant TECs. Slant TECs are integrated electron densities over the slant distance from satellite to receiver position. Figures 4a and 4b give the slant TEC comparisons for 1997–1998 annual averaged diurnal cycle between the FORTE-derived (hatched) and the IRI-ITF-predicted (black) TECs for a slant distance of 800–100 and 2000–2500 km, respectively. Figures 5a and 5b are the same except averaged over 1999–2002. On average, we found visual agreements in the amplitude and phase of the TEC diurnal cycle at low and high solar

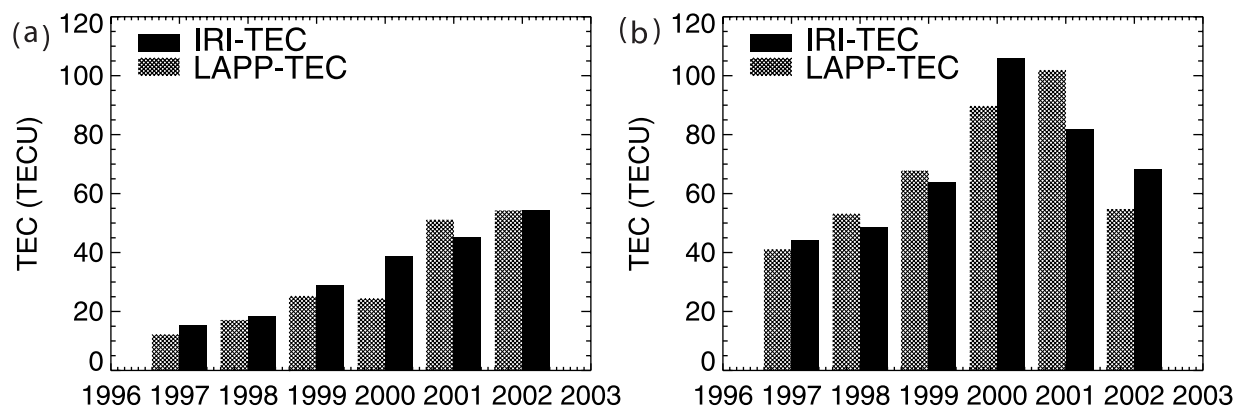


Figure 6. Slant TEC interannual variation comparisons between daytime (0800–1800 LT) FORTE-derived and IRI-ITF model-predicted averages for (a) slant distance range 800–1000 km and (b) slant distance range 2000–2500 km.

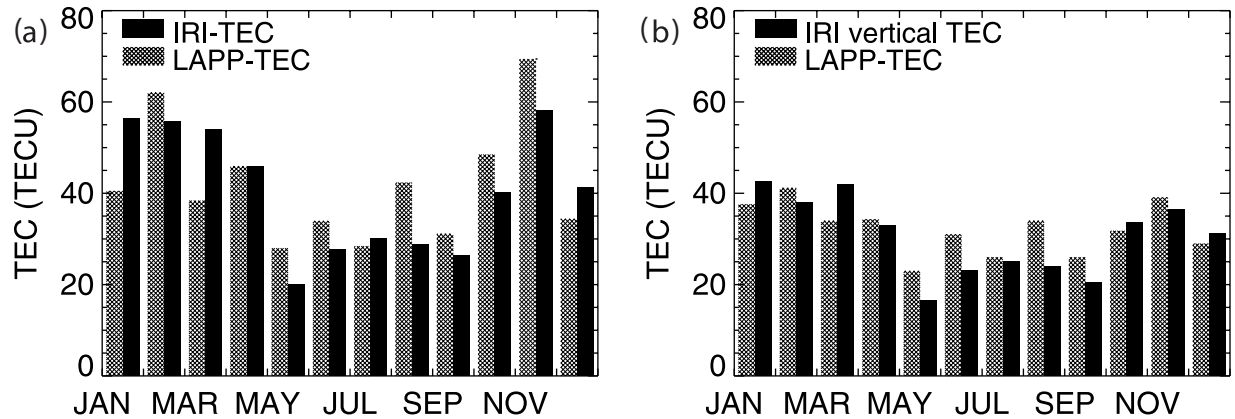


Figure 7. TEC seasonal cycle comparisons between FORTE-derived and IRI-ITF model-predicted TEC time (1100–1400 LT) for midday peak (a) slant TEC for short slant distance (800–1200 km) and (b) vertical TEC for all slant distances (800–3500 km).

activity years. The best agreements are observed at low solar activity years and short slant distances.

[16] Figures 6a and 6b compare the interannual variability of the annual mean daytime (0800–1800 LT) slant TECs between the FORTE-derived (hatched) and the IRI-ITF-predicted (black) TECs for slant distance 800–1000 and 2000–2500 km, respectively. We can see general matches between the FORTE-derived and IRI-ITF predicted TECs on an interannual timescale. Figures 7a and 7b give the seasonal variability comparisons of the 6-year (1997–2002) mean slant TECs averaged over short slant distance (800–1200 km) and mean vertical TECs averaged over all slant distances (800–3500 km) for the midday TEC peak time period (1100–1400 LT), respectively. The 6-year mean TEC

seasonal variations from the FORTE-derived and the IRI-ITF model-predicted estimations are also in good agreement in displaying characteristic semiannual seasonal cycle although relatively large differences exist for August and November.

[17] For the 27-day solar cycle TEC variability, we selected months with relatively complete monthly coverage from the FORTE-LAPP event database to conduct 4-hour (1000–1400 LT) averaged comparisons. Figures 8a and 8b give the 4-hour averaged daytime vertical TEC comparisons between the FORTE-derived and the IRI-ITF model-predicted TECs for January and July 2000, respectively. We can see general agreement during the peak phases over the 27-day solar cycle but the FORTE-derived vertical TECs (hatched) are considerably smaller

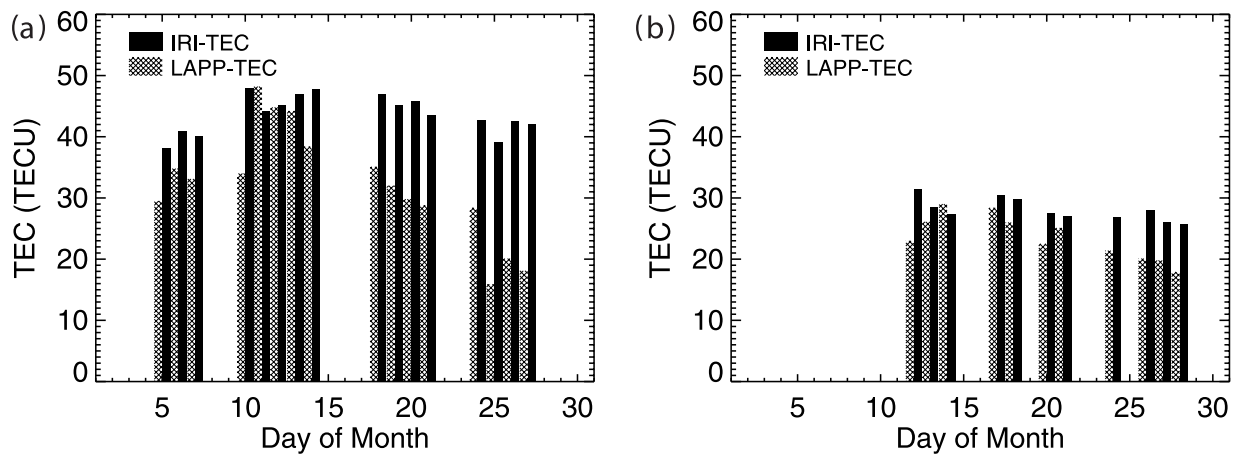


Figure 8. TEC comparisons between FORTE-derived and IRI-ITF model-predicted 27-day solar cycle for (a) 1000–1400 LT January 2000 and (b) 0800–1200 July 2000.

Table 1. FORTE-Derived and IRI-ITF Predicted Slant TEC Differences

	RMS, TECU	Percent RMS
Diurnal, 1997–1998, annual mean, 800–1000 km	0.49	4.25
Diurnal, 1997–1998, annual mean, 2000–2500 km	1.46	4.78
Diurnal, 1999–2002, annual mean, 800–1000 km	2.44	8.64
Diurnal, 1999–2002, annual mean, 2000–2500 km	2.75	4.50
Interannual, daytime annual mean, 800–1000 km	3.40	10.8
Interannual, daytime annual mean, 2000–2500 km	5.00	7.40
Seasonal, 1997–2002, 1000–1400 LT, 800–1200 km	2.54	6.29
Seasonal, 1997–2002, 1100–1300 LT, vertical TEC	1.59	4.93
27-day solar cycle, 1000–1400 LT, January 2000	13.84	36.49
27-day solar cycle, 0800–1200 LT, July 2000	5.40	20.91

than that of the corresponding IRI-ITF predicted (black) TECs during the decreasing phase.

[18] To quantitatively describe the visual agreement between the FORTE-derived TECs and the IRI-ITF model-predicted TECs, we conducted RMS error analyses. Table 1 gives the RMS and percent RMS error in the differences between FORTE-derived and the IRI-ITF model-predicted TECs for the above averaged TEC characteristics. We can see that (1) for annual mean diurnal cycle, the absolute RMS errors of slant TEC are from 0.5–1.5 TECU (low solar activity years) to 2.4–2.8 TECU (high solar activity years); (2) for daytime annual mean interannual variations, the absolute RMS errors of slant TEC are from 3.4 TECU (short slant distances) to 5.0 TECU (long slant distances); (3) for 6-year mean peak TEC time seasonal variations, the absolute RMS errors are 2.6 TECU for short slant

distances and 1.5 TECU for vertical TECs converted from all slant distances; and (4) for 4-hour averaged daytime 27-day solar cycles, the absolute RMS errors are 13.8 TECU (January 2000) and 5.4 TECU (July 2000). The relative RMS errors are from 4.2% to 10.8% for the annually averaged or multiple-year averaged comparisons while increase significantly to 20.9–36.5% for 4-hourly averaged comparisons. Therefore, quantitatively, there exists good agreement between the FORTE-derived and IRI-ITF predicted slant TEC values with a fluctuation level of smaller than 10.8% with respect to the background TEC on annual or multiple-year averaged comparisons. However, the relative differences are large for comparisons of short time averages. In the following subsection, we further examine the comparisons between the event specific FORTE-derived TECs and the IRI-model predictions.

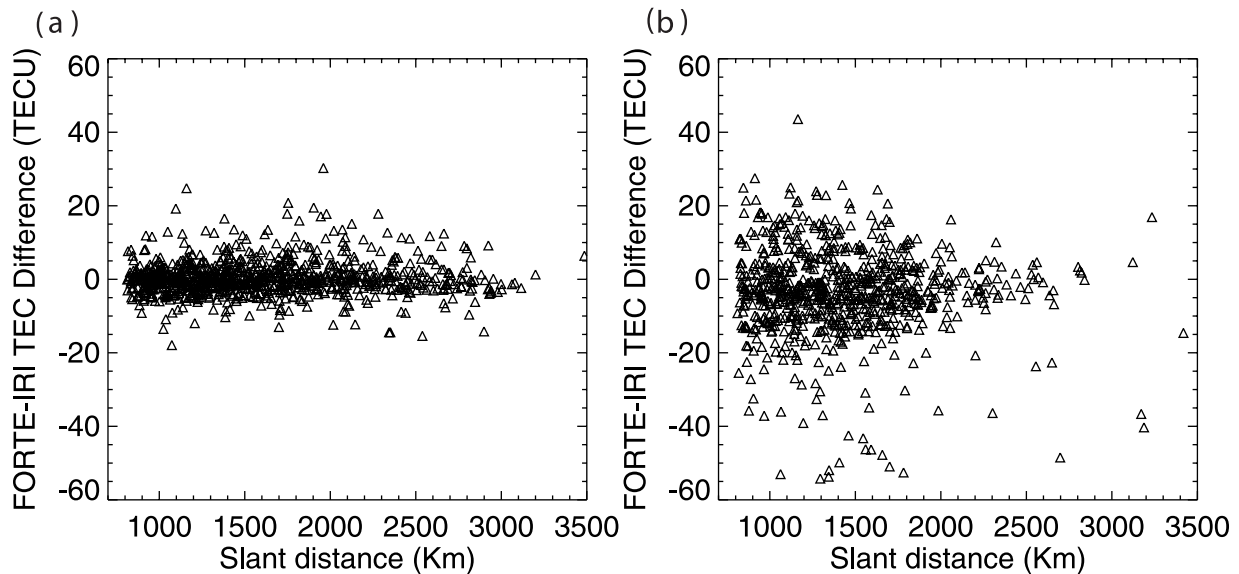


Figure 9. Event-specific differences between FORTE-derived and IRI-ITF model-predicted TECs for (a) 1997–1998 FORTE-LAPP events and (b) 1999–2002 FORTE-LAPP events.

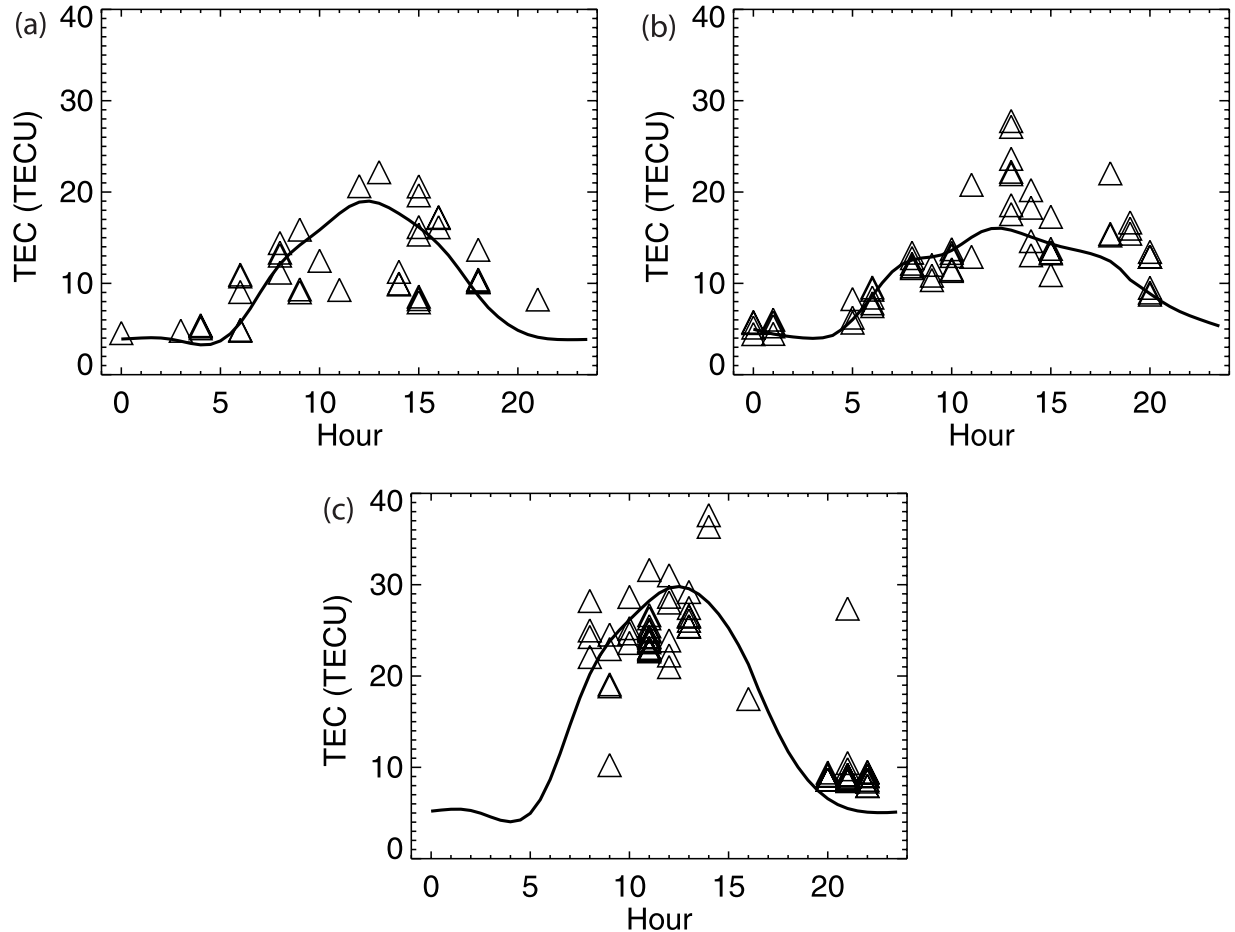


Figure 10. FORTE-IRI TEC comparisons for 1998 LAPP events: (a) January to April, (b) May to August, and (c) September to December.

2.3.2. Event-Specific Comparisons

[19] A previous study indicates that the IRI model-predicted TEC values are reasonably in agreement with the TECs obtained using global positioning satellites during daytime and geomagnetic undisturbed low solar activity periods [Wilkinson *et al.*, 2001]. Our point-to-point comparisons show that the differences between the FORTE-derived TECs and the IRI model-predicted TECs are affected by solar activity. Figures 9a and 9b give the differences in event-specific vertical TECs between the FORTE-derived (converted from slant TECs) and the IRI model-predicted TECs for low solar activity years (1997–1998) and for high solar activity years (1999–2002), respectively. The differences between the FORTE-derived TECs and the IRI-ITF model-predicted TECs are characterized by deviations from the near-zero averaged difference, suggesting reasonable matches on average. We believe that such deviations are more likely due to the lack of topside ionosphere data

used in the IRI model in addition to day-to-day TEC fluctuations that the model is not able to resolve. However, the deviations are much larger for high solar activity years than those of low solar activity years, implying a limitation for using the IRI model in predicting realistic transient TECs for high solar activity years.

[20] In addition to the contributions of solar activity to the differences between the FORTE-derived and the IRI-ITF model-predicted TECs examined on annual basis, further examinations indicated that such differences are also seasonally and time of day dependent. We selected 1998, the year with relatively more seasonal and diurnal data coverage, to explore seasonal and diurnal characteristics of the differences. Figures 10a–10c show how FORTE event-specific vertical TECs are compared with the IRI model-predicted vertical TECs on the diurnal variations for January–April 1998, May–August 1998, and September–December 1998, respectively, where the solid line denotes IRI model-predicted vertical TEC

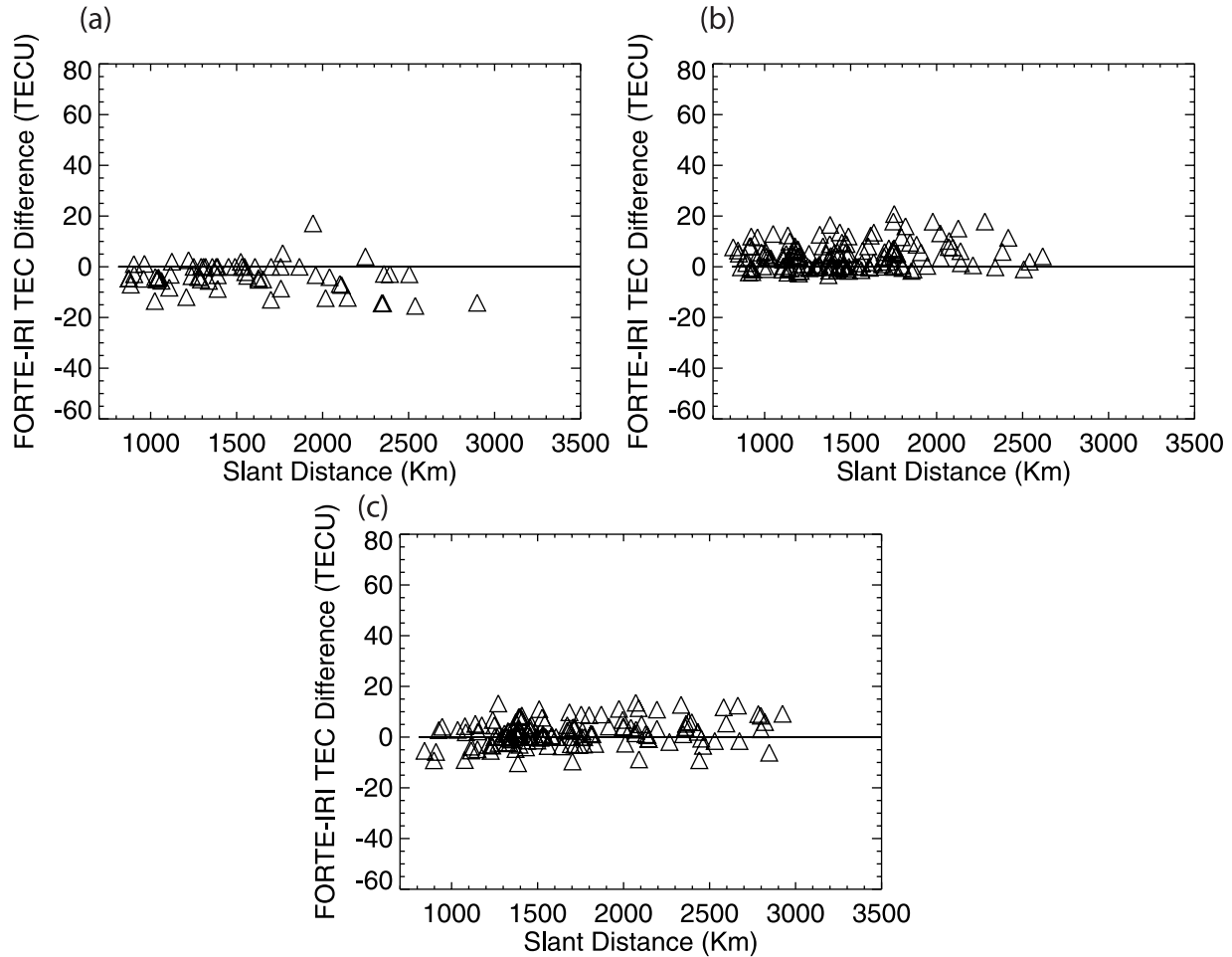


Figure 11. FORTE-IRI TEC differences during peak TEC time (1000–1400 LT), 1998 for (a) September to December, (b) May to August, and (c) January to April.

diurnal variations and the triangles are the FORTE event-specific vertical TECs. In order to eliminate the slant distance impact as discussed by *Huang and Roussel-Dupré* [2005], the selected FORTE events are constrained within 800–1000 km (extended to 1400 km for the September–December case to include enough events for analysis).

[21] We can see from Figure 10 that the FORTE event-specific vertical TEC generally follows the IRI model-predicted diurnal variations for the two semiannual seasonal high-TEC phases (January–April and September–December) and the major summer seasonal low-TEC phase (May–August). However, large deviations most likely existed during the midday peak TEC time period (1000–1300 LT). In particular, there seem to exist biased differences during May–August, when the IRI model-predicted vertical TECs are consistently lower than the FORTE-derived TEC values (Figure 10b). To

explore any possible biased differences, we examined the seasonal differences during midday peak TEC time period (1000–1400 LT).

[22] Figures 11a–11c give the differences between the FORTE-derived vertical TECs and the IRI-ITF model-predicted TECs during midday peak TEC time (1000–1400 LT) for the three TEC seasonal phases in 1998. Interestingly, we found that although we have seen deviations over near-zero averages on an annual basis, there exist marked seasonal differences. Positively biased differences, where the IRI model underpredicts TECs, existed for the summer seasonal low-TEC phase (Figure 11b). Negatively biased differences, where the IRI model overpredicts TECs, were observed for winter–spring semiannual high-TEC phase (Figure 11c). No biased differences were found for the second semiannual seasonal TEC high phase (Figure 11a). The results suggest

Table 2. FORTE-Derived and IRI-ITF Predicted TEC Point-to-Point Differences

	RMS, TECU	Percent RMS
1997–1998 daytime (800–1800 LT)	12.6703	56.9055
2000–2001 daytime (800–1800 LT)	22.5132	79.9247
1998 Jan–Apr (1000–1400 LT)	7.09434	29.2588
1998 May–Aug (1000–1400 LT)	6.93978	18.8845
1998 Sep–Dec (1000–1400LT)	5.50026	11.3509

that while the IRI model predicts reasonable annually averaged TECs it may overpredict seasonal variations.

[23] Table 2 gives RMS error analysis results showing quantitative comparisons between the event specific FORTE-derived TECs and the IRI-ITF model predictions for high and low solar activity years, and different seasons for 1998. As expected the RMS errors are much larger when compared event specifically than compared on annual or multiyear averaged. Instead of percent RMS of smaller than 10.8%, as high a value as 79.9% is found. We can see from Table 2 that the differences between the FORTE-derived TECs and the IRI-ITF model predictions are much larger for high solar activity years (79.9% RMS) than those for low solar activity years (56.9% RMS) for daytime (0800–1800 LT). Nighttime data are not available for FORTE TECs during high solar activity years 2000–2001. Seasonal differences are also observed at peak TEC hour (1000–1400 LT), where the percent RMS errors are largest (29.3%) for January to April and smallest (11.4%) for September to December with a medium value of 18.9% for May to August.

[24] In conclusion, our FORTE-derived TEC variabilities reasonably match the IRI model predictions in describing characteristic TEC variabilities when compared for annual or multiyear averages with smaller than 10.8% RMS errors. As large as 79.9% RMS error is found at high solar activity years when compared event specifically. Given that the IRI-ITF model predicted TECs are values based on climatology data, the differences in RMS between the small errors on average and the large errors for event-specific comparisons imply that day-to-day variations are large at Los Alamos, especially during high solar activity years. Our results also revealed that the IRI model may underpredict daytime TEC during summer and overestimate TEC during winter–spring months.

3. Comparisons With GPS-Derived TECs

3.1. GPS Satellite and TEC Measurements

[25] The architecture of the Global Positioning System (GPS) [Hoffmann-Wellenhof *et al.*, 1997] was developed in the mid-1970s. It is a constellation of satellites intended to provide precise positional information at

points on and above the Earth’s surface. The satellites are in 12-hour circular orbits at altitude 20,200 km inclined at 55° to the equator. Between four and eight satellites are visible above 15° elevation at any time from any location on the Earth’s surface. The satellites carry precision time and frequency standards and transmit L band signals at 1227.60 MHz (L1) and 1575.42 MHz (L2). The GPS position fixing makes use of the propagation time delays and takes into account the differential time delays on the two frequencies due to the presence of the plasmasphere. Because of the differential time delay on L1 and L2, the GPS satellites have been applied to measuring the TEC through the ionosphere and protonosphere between the satellite and a receiver at the ground [Lanyi and Roth, 1988].

[26] Many GPS receivers have been developed and distributed since the solar maximum in 1989 and have provided continuous and worldwide coverage presented in the form of TEC maps. It has been indicated that the GPS-derived TEC map has the best global TEC representation at any latitude and longitude in quiet geomagnetic days, while it provides a mean representation of ionosphere in disturbed magnetic activity days [Meza *et al.*, 2002]. Incoherent scatter radar has been used as a calibration tool to evaluate TEC values from GPS measurements [e.g., Makela *et al.*, 2000; Liliensten and Cander, 2003]. It has been shown that the GPS technique gives very good results on nighttime TECs for both quiet and disturbed geomagnetic conditions while in some cases there are daytime underestimations of the GPS-deduced TEC. General agreement has been found between GPS-deduced TECs and other TEC estimates for various locations at midlatitudes for the solar maximum week of 23–28 April 2001 using a regularized estimation algorithm combining signals from all GPS satellites for a given instant and a given receiver, especially for quiet geomagnetic conditions [Arikan *et al.*, 2003].

[27] The GPS-deduced TEC techniques are subject to some problems. First, the algorithms and software used for TEC calculations impose different biases. Second, a number of satellites observed at any one time are in different parts of the sky and the TEC varies both spatially and temporally. Furthermore, the GPS measured slant TEC values along different paths of available GPS satellite links have to be converted to equivalent vertical GPS TECs. In the midlatitudes, where the TEC normally shows a smooth spatial variation, this conversion can be performed in terms of a geometrical parameter.

[28] Two GPS TEC data sources are used in this study. First, the vertical GPS TEC maps from the National Oceanic and Atmospheric Administration (NOAA). Second, the line of sight GPS TEC measurements observed by two Allen Osborne Associates (AOA) ICS-4000Z GPS receivers at Los Alamos. The slant FORTE TECs used here are those derived with the quartic

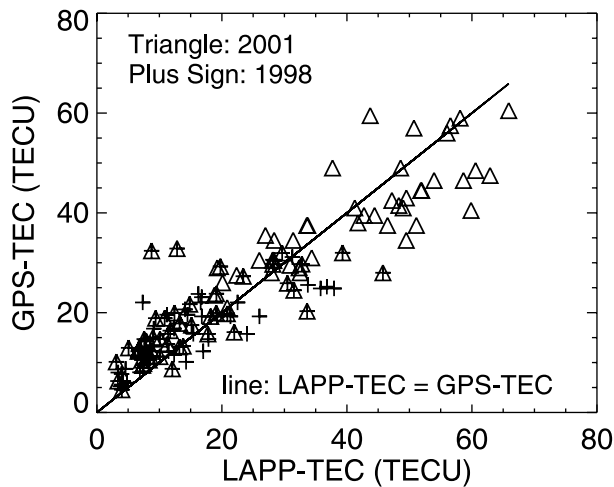


Figure 12. Comparisons of FORTE-derived (with quartic effects) and NOAA GPS TECs for 1998 (pluses) and 2001 (triangles) half-hour averaged FORTE events.

term included and the Earth's curvature effects are also included in converting the slant TEC to the vertical TEC.

3.2. Comparisons With NOAA U.S. TEC Map Estimations

[29] The United States GPS TEC maps generated from NOAA for low (1998) and high (2001) solar activity years were used to compare with our FORTE-derived TEC results. The NOAA GPS TECs are derived from the observations of GPS receivers in the Continuously Operating Reference System (CORS) network. At each site a best fit zenith TEC is derived and the U.S. TEC maps are generated by a closest three-site triangular interpolation at a temporal resolution of half an hour. Since the FORTE-derived TECs are at 1-min temporal resolution, we calculated the TEC averages of all the available FORTE events over half an hour period of time in order to compare with the NOAA GPS TECs. Since Los Alamos is not a CORS site the corresponding NOAA GPS TEC values at Los Alamos are estimated from the maps by spatial interpolation.

[30] Figure 12 gives comparisons between the half-hourly FORTE event-averaged TECs and the corresponding GPS-estimated TECs for a low solar activity year (1998) and for high solar activity year (2001), respectively. In Figure 12, the straight line indicates the location where the FORTE TEC equals GPS TEC, and the differences between the FORTE TEC and GPS TEC are shown as the distance of triangle symbols to the straight line, where triangles are for 2001 data and pluses are for 1998 data. Overall, our FORTE-derived TECs with quartic effect included reasonably

support the GPS TECs estimated from NOAA TEC maps despite of the uncertainties resulting from spatial interpolations in the GPS TEC estimations. Nevertheless, for the two years (1998 and 2001) examined, we found that our FORTE-derived TECs tend to be consistently smaller than the GPS TEC estimations for very small TECs (<10 TECU) and predominantly larger than the GPS TEC estimations for very large TECs (>40 TECU). Whether such differences are due to simple spatial extrapolations or there is some missing factors in either NOAA's GPS TEC or FORTE TEC estimations or both, is something that requires further investigation. In the next section, we will use local GPS TEC measurements, which are not subject to spatial extrapolations, to do further comparisons.

3.3. Comparisons With Local GPS TEC Measurements

[31] The GPS TEC measurements from two AOA ICS-4000Z GPS receivers, mounted at the Physics Building at Los Alamos National Laboratory, are also used to compare with the corresponding FORTE-derived TECs. The ICS-4000Z GPS receiver is optimized for precision measurement of the ionosphere's TEC with simultaneous and independent digital tracking of up to eight satellites. It produces very accurate pseudorange and carrier phase measurements from the L1 C/A code and P code and from the L2 P code. In addition, the receiver corrects ionospheric errors in the presence of the encrypted P code. The receiver determines the line of sight TEC calculated from the differential (L1-L2) group time delay by cross-correlated time lag and differential carrier phase.

[32] The AOA GPS slant TEC data partially overlaps with FORTE data for five months: March, July, and December 2001 and March and June 2002. The data are collected from 32 GPS satellites at elevation angles greater than 15° with a temporal resolution of 10 s. The GPS TECs are measured to the satellite height of 20,200 km, which include contributions from the protonosphere (above 1000 km). The protonospheric TECs are derived from the ionosphere through vertical diffusion. Typical variations in the protonospheric TEC are observed as a result of the daytime upward diffusion and nighttime downward diffusion in the ionosphere. The protonospheric TEC also varies with season, 11-year solar cycle, and with location. Magnetic storms have large effects on the fluctuations of the protonospheric TEC. At Salisbury (34.77°S , 138.63°E) in southern Australia, close to zero protonospheric TECs are observed in winter while values large than 15 TECU are observed in equinoctial months [Breed *et al.*, 1995]. To estimate and remove the contributions from the protonosphere for the AOA GPS TEC, we adopted a median value of 2 TECU at Boulder, Colorado,

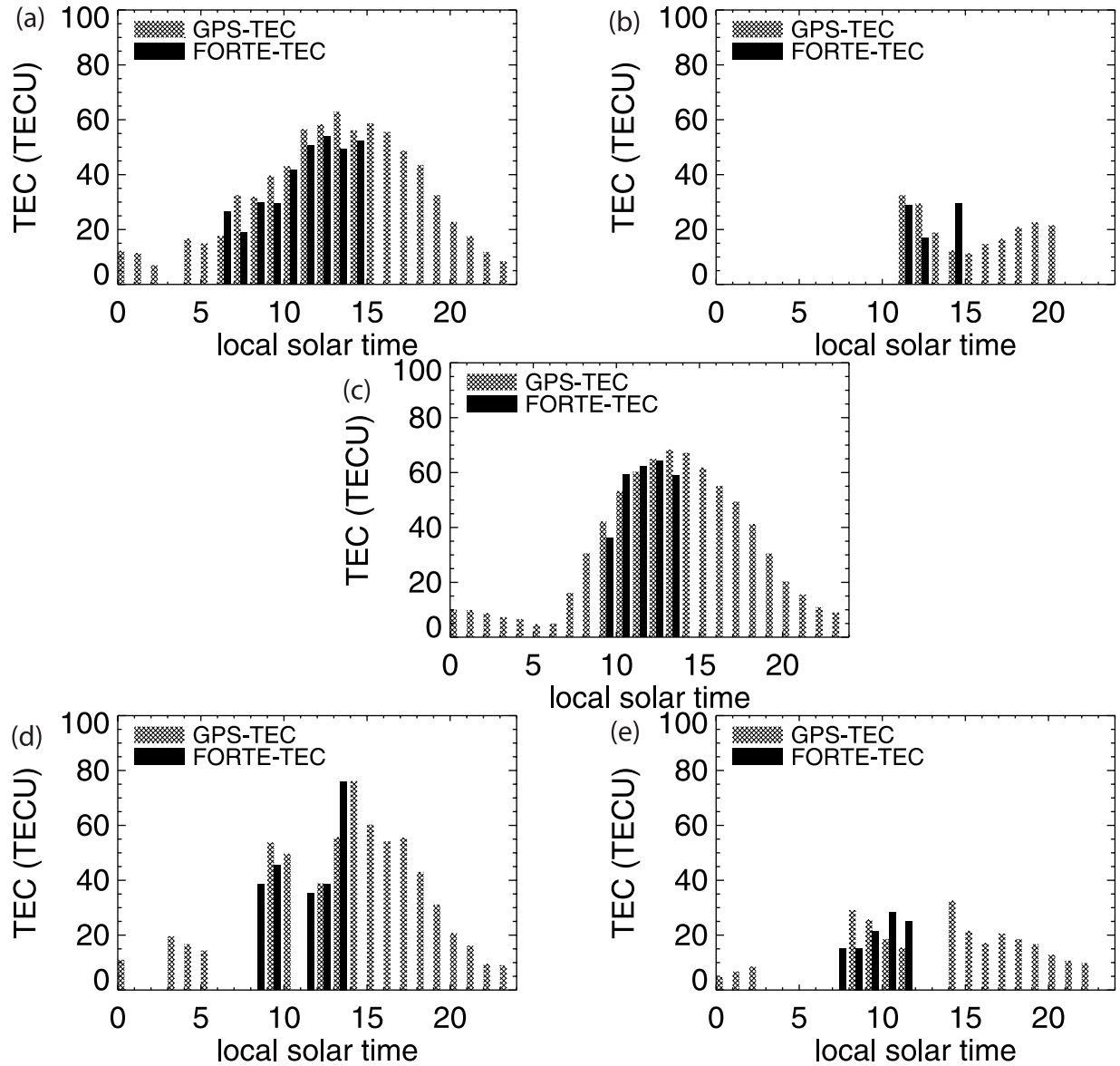


Figure 13. Comparisons of FORTE-derived (black) and AOA GPS (hatched) TECs for (a) March 2001, (b) July 2001, (c) December 2001, (d) March 2002, and (e) June 2002.

derived from a geostationary satellite (35,000 km) [Kersley and Klobucher, 1978] and applied a diurnal cycle with a daytime peak of 3 TECU and a nighttime low of 1 TECU to the AOA GPS TEC data. The slant ionospheric TECs are converted to vertical TECs with the Earth's curvature effects included assuming a peak electronic density height of 350 km. The effects of different peak electronic density heights, along with the effects of elevation angle and individual satellite biases, on GPS TEC measurements are discussed.

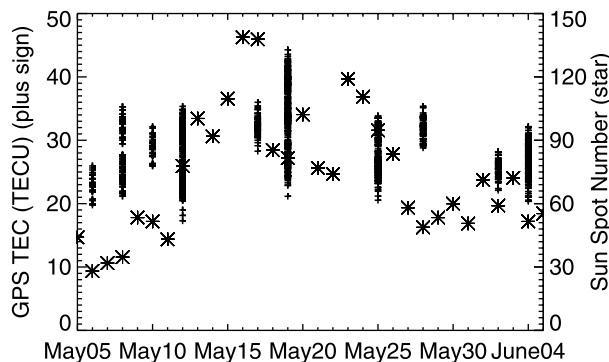
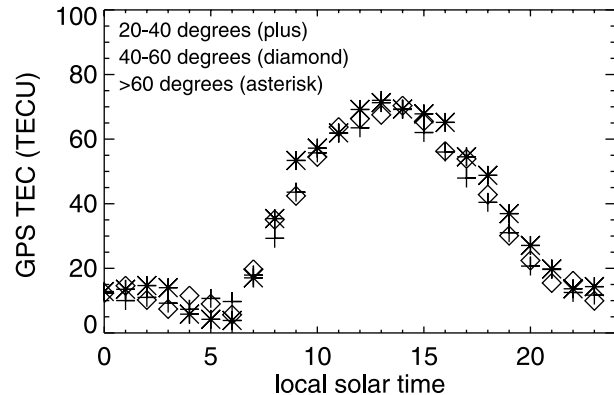
[33] Our results show good agreement on hourly averaged TEC diurnal cycle and seasonal variations between the AOA GPS TEC and FORTE-derived TEC. Figures 13a–13e give hourly mean vertical TEC comparisons between the FORTE-derived and the AOA GPS measurements (with elevation angle $>20^\circ$) for the five months. We can see that there are no biased differences in the magnitude of TEC except for March 2001, where the AOA GPS TECs are consistently larger than the corresponding FORTE TECs. Note that the vertical AOA

Table 3. FORTE-Derived and AOA GPS TEC Monthly Mean Differences

	Mar 2001	Jul 2001	Dec 2001	Mar 2002	Jun 2002
RMS	2.3173	6.0581	2.3219	2.8263	3.2869
Percent RMS	5.7644	29.842	4.6253	6.2253	16.353

GPS TECs are derived from the slant TECs assuming a peak electronic height of 350 km. We found that the only date that was used to calculate the mean AOA GPS TECs for the March 2001 case is 13 March, when the available data at Boulder show that the peak electronic density height is around 220 km. We found that the apparently biased TEC magnitude may be corrected by using of the “real-time” peak electronic density height to some extent but not enough to fully remove the biases. This may imply that the contributions from the protonosphere are probably underestimated for that particular day.

[34] The RMS error analyses (Table 3) show that at the spring and autumn-winter semiannual TEC peak phase months (March and December), the FORTE and AOA GPS TECs match well in half-diurnal (daytime only, no nighttime FORTE data available) variations. The relative RMS errors are 5.8%, 4.6%, and 6.2% for March 2001, December 2001, and March 2002, respectively. For the summer low TEC phase months (June and July), while both data are unfortunately not enough to describe diurnal variations it can be seen that the magnitude of the FORTE-derived TECs is consistent with that of the AOA GPS TECs. Furthermore, RMS analyses indicate poor matches with large RMS error of 29.8% (July 2001) and 16.4% (June 2002). We also noticed unreasonable variations during daytime before noon for summer months in the AOA GPS TEC data, where TEC decreases when TEC should increase in the increasing

**Figure 14.** AOA GPS TEC (pluses) variations over 27-day solar cycle for 1300–1400 LT from 5 May to 4 June 2004, pseudo random noise code = 15, and elevation angle $>60^\circ$. Asterisks are daily sunspot numbers.**Figure 15.** Elevation angle impact on AOA GPS TECs with elevation angles of 20° – 40° (pluses), 40° – 60° (diamonds), and $>60^\circ$ (asterisks).

phase of the diurnal cycle. Nevertheless, the magnitude of the AOA GPS TEC values for the two summer months are comparable to that from FORTE-derived TECs, indicating reasonable agreement in TEC seasonal variations between the FORTE-derived and the AOA GPS TECs.

[35] For comparisons of the 27-day solar cycle TEC variations, we used AOA GPS TEC data for May–June of 2004. Figure 14 shows AOA GPS TECs (pluses) from 5 May to 4 June 2004 during peak TEC time from 1300 to 1400 local solar time, also given are daily sunspot numbers (shown as asterisks). We can see that for sunspot number varying from 30 to 140 (a sunspot number increase of 110), the peak time TEC varies from about 23 to above 35 (a TEC increase of 12 TECU). Compared to our earlier analysis [*Huang and Roussel-Dupré, 2005*], we found comparable TEC variability on the 27-day solar cycle. The averaged FORTE TEC varies from smaller than 20 TECU to above 30 TECU (a TEC increase of greater than 10 TECU) for sunspot number changes from 150 to 270 (a sunspot number increase of 120) for July 2000 [*Huang and Roussel-Dupré, 2005, Figure 8b*]. Given that the year 2000 is a high solar activity year while the year 2004 is a low solar activity year, more data are needed to confirm if the magnitude of the TEC variability on the 27-day solar cycle at high solar activity years is comparable to that at low solar activity years.

[36] To evaluate the impact of elevation angle on the AOA GPS TEC measurements, we examined vertical TECs derived from GPS data with different ranges of elevation angles. Figure 15 demonstrates the impact of the elevation angles (20° – 40° , 40° – 60° , and $>60^\circ$) on derived TECs using the data of 12 December 2001 assuming a mean electronic density height of 350 km. No biased impacts on the derived vertical AOA GPS

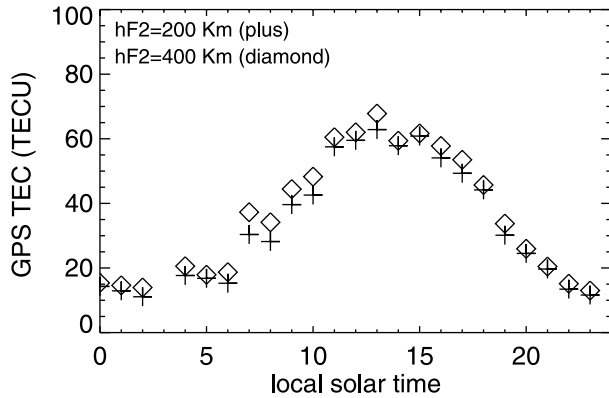


Figure 16. Peak electron density height (hF_2) impact on AOA GPS TECs for $hF_2 = 200$ Km (pluses) and $hF_2 = 400$ km (diamonds).

TECs are found by using different ranges of elevation angles.

[37] We examined the impact of the peak electronic density height on the vertical TECs converted from slant TECs with the Earth’s curvature effects included. Figure 16 gives an example for 13 March 2001, showing the vertical TECs with a peak electronic density height of 200 km (diamonds) and those of 400 km (pluses). We can see that the derived vertical TECs are reduced as a result of reducing the peak electronic density height. The differences in derived vertical TECs can be as high as 10 TECU (or 25%) on a background TEC of 40 TECU for the difference of 200 km in the use of peak electronic density height.

[38] The relative location of satellites with respect to the receiver, hence the ray pass direction traversing different ionospheric zones, imposes different biases on the GPS TEC measurements. To evaluate possible biases on the AOA GPS TECs from such effect, we examined AOA GPS TECs derived from 32 individual GPS satellites for 12 December 2001. Figures 17a and 17b give the TECs derived from the 32 satellites with elevation angles greater than 20° , and the relative differences (percent standard deviations with respect to the mean), respectively. During each 1-hour period of time there are up to eight GPS satellites simultaneously being observed and used to derive GPS TECs. The results indicate that the amplitude of the TEC diurnal cycle can be affected by using individual GPS satellites. As seen from Figure 17a, the absolute TEC differences are about 15–20 TECU throughout the day. The midday peak TEC changes from about 80 TECU to below 65 TECU. The TEC low at midnight can vary from 20 TECU to below 5 TECU from using different GPS satellites. We can see that the relative changes due to using different satellites (Figure 17b) are much larger during nighttime (20–60%) than during daytime (less than 10%). Therefore the GPS TECs derived as such need to include observations from as many satellites as possible in order to come up with the characteristic TECs not subject to the biases due to a particular ray pass by a single satellite.

4. Comparisons With Ionosonde Observations

4.1. Ionosonde Data Description

[39] The ionosonde is a vertical incidence sounding radar utilizing high-frequency radio waves to probe the

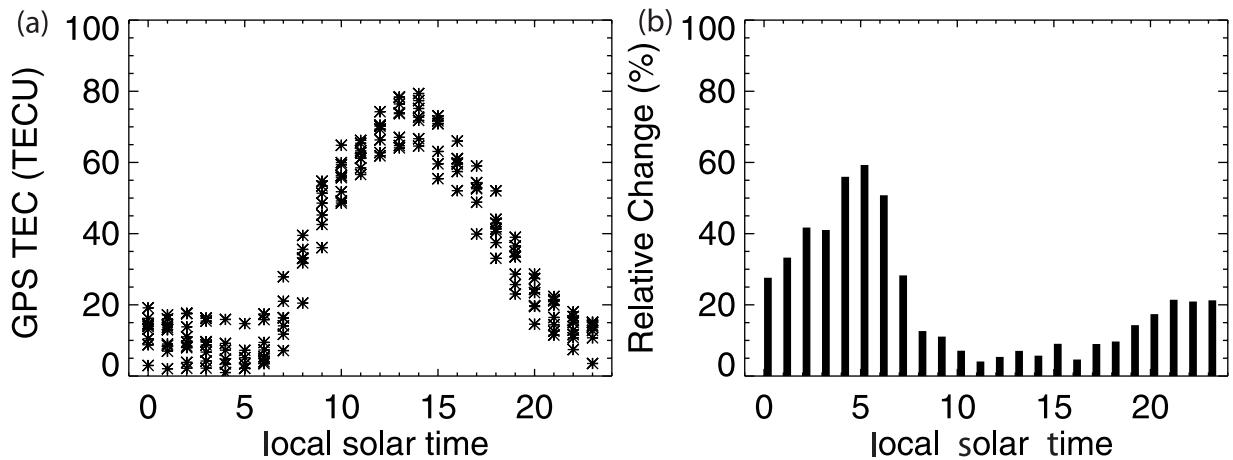


Figure 17. Hourly averaged AOA GPS TECs derived from 32 individual satellites for 12 December 2001 (a) absolute TEC differences (TECU) and (b) relative TEC differences (%).

ionosphere from about 90 to 900 km. It has been used for measurements of the terrestrial ionosphere for more than 70 years. Over time, ionosondes have become increasingly more sophisticated in capability, more reliable in operation, and of greater scientific utility [Wright, 1969; Paul, 1991]. At the present time, 174 ionosondes are operational worldwide according to the Space Environment Center at NOAA.

[40] An ionosonde transmits a range of radio wave frequencies vertically, typically from 0.1 to 30 MHz. The path of a radio wave is affected by the refractive index of the ionosphere. The refractive index is inversely proportional to the frequency of the transmitted wave. As the frequency increases, each wave is refracted less by the ionization in the layer and penetrates further before it is reflected. Eventually, a frequency is reached that enables the wave to penetrate the layer without being reflected. An ionosonde measures the time of flight for each frequency to be reflected from the various ionized layers in the ionosphere, the strength of the reflection, and the height at which a frequency can be reflected. These ionosonde measurements can be used to determine ionization density profile and to derive ionospheric TEC [Union Radio Scientifique Internationale, 1993].

[41] The ionosonde data used in this study are obtained from World Data Center for Solar-Terrestrial Physics at the Rutherford Appleton Laboratory. We selected Boulder, Colorado (40.0°N, 105.2°W), which is the closest station where data are available for the FORTE data period from 1997 to 2002 with temporal resolutions of 1 hour (1997–1999) and 15 min (2000–2002). Correlation studies are performed on the variability of the critical frequencies for F_2 layer from the Boulder ionosonde measurements and that of the FORTE-derived TECs at Los Alamos on diurnal, seasonal, and interannual timescales.

4.2. Relationship Between TEC and Critical Frequencies

[42] The limiting frequency at or below which a wave component is reflected by, and above which it penetrates through, an ionospheric layer at vertical incidence is known as the critical frequency of that layer. The critical frequency is simply a function of electron density. In the case of the ordinary wave, the critical frequency is related to the electron density by the relation: $F_c = 8.98 \times \sqrt{N_e}$. Here F_c is the critical frequency in Hz, N_e is the electron concentration in el/m^3 . In the case of the extraordinary wave, the magnetic field has an additional effect, and reflection occurs at a frequency that is higher than the ordinary mode by half the electron gyrofrequency.

[43] The greatest contribution to the TEC is from the F_2 layer, which is a highly variable ionized region where the electron concentration and distribution is governed

by solar activity, geomagnetic influences, and neutral wind effects. The F_2 layer critical frequency, f_oF_2 , has been used as an index to neural network TEC predicting models up to 7 days ahead very successfully. Some researches indicated that TEC and f_oF_2 display very similar temporal variation patterns in general at both geomagnetically quiet and disturbed times [e.g., Ma and Maruyama, 2002]. It has also been found that f_oF_2 is highly variable on timescales from decades to seconds with the occurrence of ionospheric disturbances associated with geomagnetic storms [e.g., Cander et al., 2004]. Given the temporal resolution of our FORTE-derived TEC data and the ionosonde critical frequency measurement data recorded hourly (every 15 min after the year 2000), we investigated the correlations between the FORTE-derived TEC and the critical frequencies of F_2 layer for low and high solar activity years and for quiet and disturbed geomagnetic conditions.

4.3. Correlations Between FORTE-Derived TEC and Ionosonde F_c Measurements

[44] The ionosonde critical frequency measurements for the F_2 layer at Boulder are examined. The results are used to describe the F_2 layer characteristic seasonal and diurnal variations. The correlations are computed between the F_2 layer critical frequency and the FORTE-derived TECs for low and high solar activity years, for different phases of seasonal cycle, for daytime and nighttime, and for quiet and disturbed geomagnetic conditions.

[45] Figures 18a–18d give F_2 region critical frequency diurnal variations for March (seasonal high phase) and July (seasonal low phase) of 1998 (low solar activity year) and 2001 (high solar activity year), respectively. In the F_2 region, during the semiannual high-TEC phases the critical frequency has one well-developed peak around noon. During the summer low-TEC phase the critical frequency features a flattened daytime high plateau with double peaks at around 0800–0900 and 1500 local solar time. The seasonal variations in the F_2 region critical frequency are shown for the three periods of time, after midnight (Figure 19a), during midday peak (Figure 19b), and before midnight (Figure 19c). It has been shown that the daytime semiannual cycle observed in TEC seasonal variations existed for all the three periods of time for the F_2 region critical frequency with seasonal high phases peaked at March–April and October–November and a major seasonal low phase in summer months. Furthermore, the amplitude of such a semiannual seasonal cycle in the F_2 region critical frequency is the greatest during the period of time before midnight.

[46] We know that the largest contribution to the ionospheric TEC is from the F_2 region and that there exists a relationship between the F_2 region critical

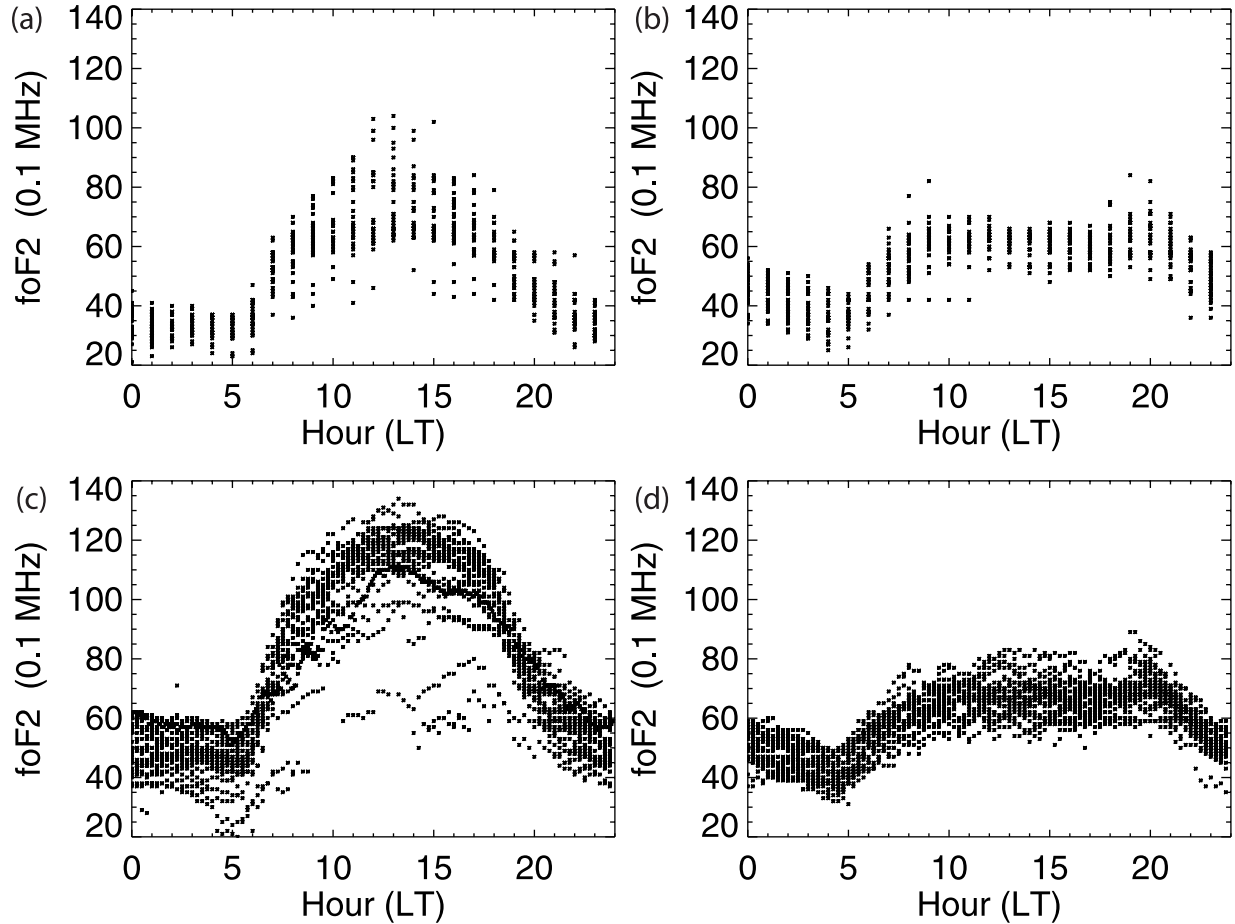


Figure 18. Diurnal variations of F_2 region critical frequency ionosonde measurements at Boulder for (a) March 1998, (b) July 1998, (c) March 2001, and (d) July 2001.

frequency squared, $(f_oF_2)^2$, and the ionospheric TEC. Figures 20a–20d compare the variations of FORTE-derived TEC (triangles) and the corresponding $(f_oF_2)^2$ (asterisks) plotted over diurnal, seasonal, interannual timescales, and the 27-day solar cycle, respectively. We can see that the two variables display similar temporal variations revealing major characteristics of the diurnal cycle, seasonal cycle, the 11-year solar cycle, and the 27-day solar cycle. Both the FORTE-derived TEC and the $(f_oF_2)^2$ show a diurnal cycle peaked at local solar noon, a semiannual seasonal cycle with double highs observed around March and November, a half 11-year solar cycle of increasing trend following increases in solar activity from 1997 to 2002, and a 27-day solar cycle during daytime for April 2001.

[47] Table 4 gives the correlation coefficients between FORTE-derived TEC and $(f_oF_2)^2$. We can see that the TEC and critical frequency squared correlations are also related to solar activity and geomagnetic condition. For

all-season combined data, compared to the low solar activity year (1998) the correlation coefficients are reduced significantly (from 0.63 to 0.35) for high solar activity year (2001) during daytime while has increased slightly during nighttime (from 0.45 to 0.55). The correlation coefficients at nighttime (0.73–0.92) are greater than those during the day (0.49–0.62) for data seasonally sampled. Furthermore, the correlation coefficients for geomagnetic storm conditions ($0.89–0.96$, $Kp > 5$) are greater than geomagnetic quiet conditions ($0.72–0.78$, $Kp < 4$).

[48] To explore possible seasonal, time of day, and solar activity dependence in the linear relationships between the FORTE-derived TEC and the F_2 region critical frequency, we computed linear curve fitting functions in various cases for cold season (September–April), warm season (May–August), daytime peak TEC period (1000–1400 LT), nighttime (1800–0800 LT), low solar activity year (1998), and high solar activity year

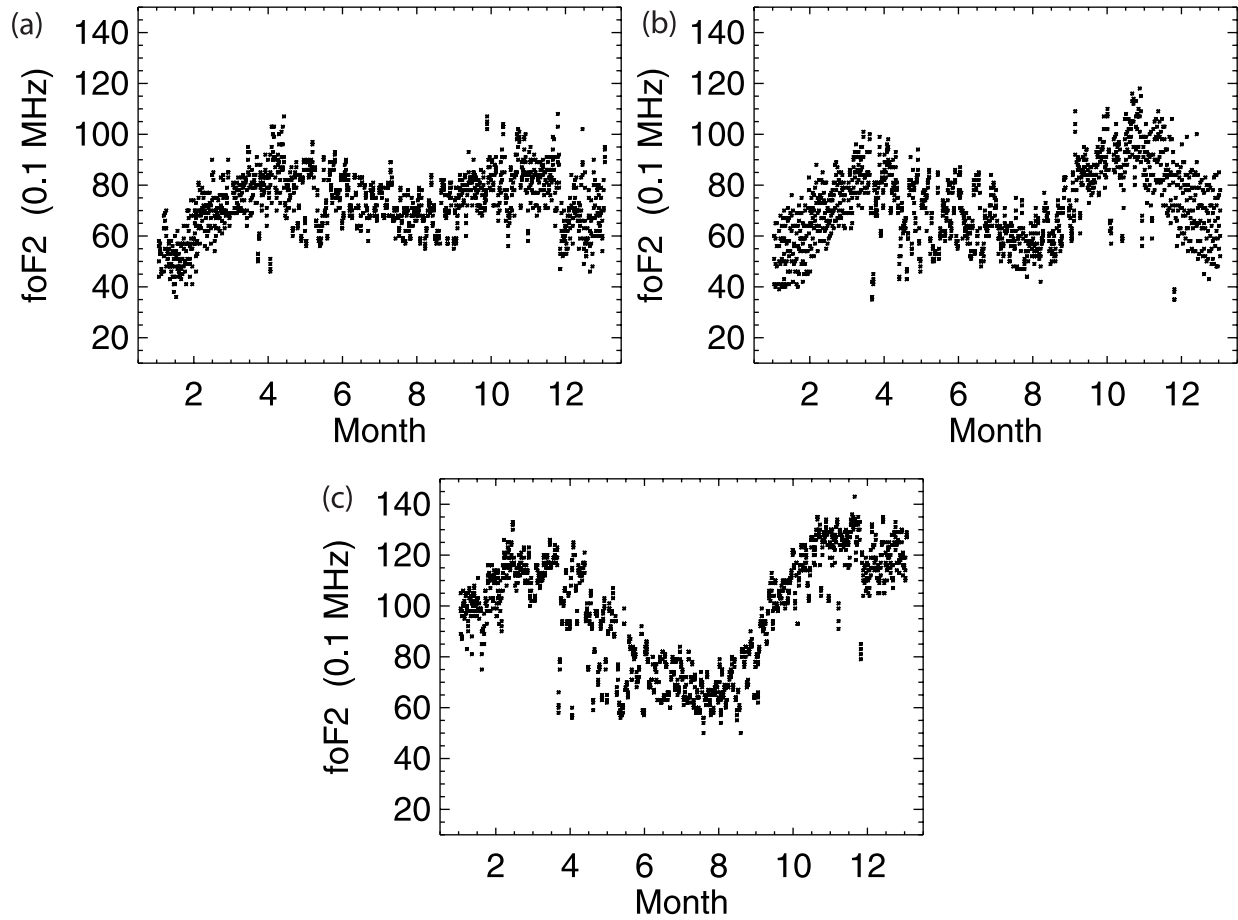


Figure 19. Seasonal variations of F_2 region critical frequency ionosonde measurements at Boulder for 2001 during (a) 0100–0200 LT, (b) 1300–1400 LT, and (c) 2200–2300 LT.

(2001). We define the linear curve fitting function: $y = ax + b$, where y is the FORTE-derived TEC (in TECU), x is the F_2 region critical frequency squared, or $(f_oF_2)^2$ (f_oF_2 is in units 0.01 MHz), and a , or dy/dx , is the linear change rate of TEC as a function of $(f_oF_2)^2$. Figures 21a–21f show the results with the data plotted in black stars and their linear fits plotted with the straight line. Table 5 gives the offset, b , and the slope, dy/dx , from the linear curve fittings, as well as RMS and percent RMS with respect to the original data. Also given in Table 5 are correlation coefficients between TEC and $(f_oF_2)^2$.

[49] We can see that the range of the percent RMS errors is relatively stable at 22–35%. Real-time comparisons with the ionosonde network have been conducted with the University of Alaska at Fairbanks (UAF) Eulerian parallel polar ionosphere model for Boulder, Colorado, during a period from May 2004 to March 2005 (S. Maurits et al., Real-time UAF Eulerian parallel polar ionosphere model: Real-time comparisons with the ionosonde network, 2005, available at [http://www.arsc.](http://www.arsc.edu)

http://www.arsc.edu/SpaceWeather/rt_compar.htm). Their comparisons are made between the ionosonde f_oF_2 and the f_oF_2 evaluated from the peak electron density from the model simulated 3-D electron density profile on the basis of a single data fit function. Their results indicate smaller daytime percent RMS errors of 9–23% and larger nighttime percent RMS errors of 16–47%. While our RMS errors fall in the range the UAF model presented the daytime and nighttime differences are not observed in our results. The reason for this is probably that we allow data to derive a data-dependent fit function instead of using a single prescribed f_oF_2 and TEC (or N_e) relationship function. We found that such functions are seasonal and time of day dependent. The slope is larger in warm season than that in cold season for both low and high solar activity years; that is, for a given increase in f_oF_2 , TEC increases more in warm season than in cold season. Also, the slope is larger during daytime than that during nighttime for low solar activity year (1998) (no nighttime data are available for high solar activity years).

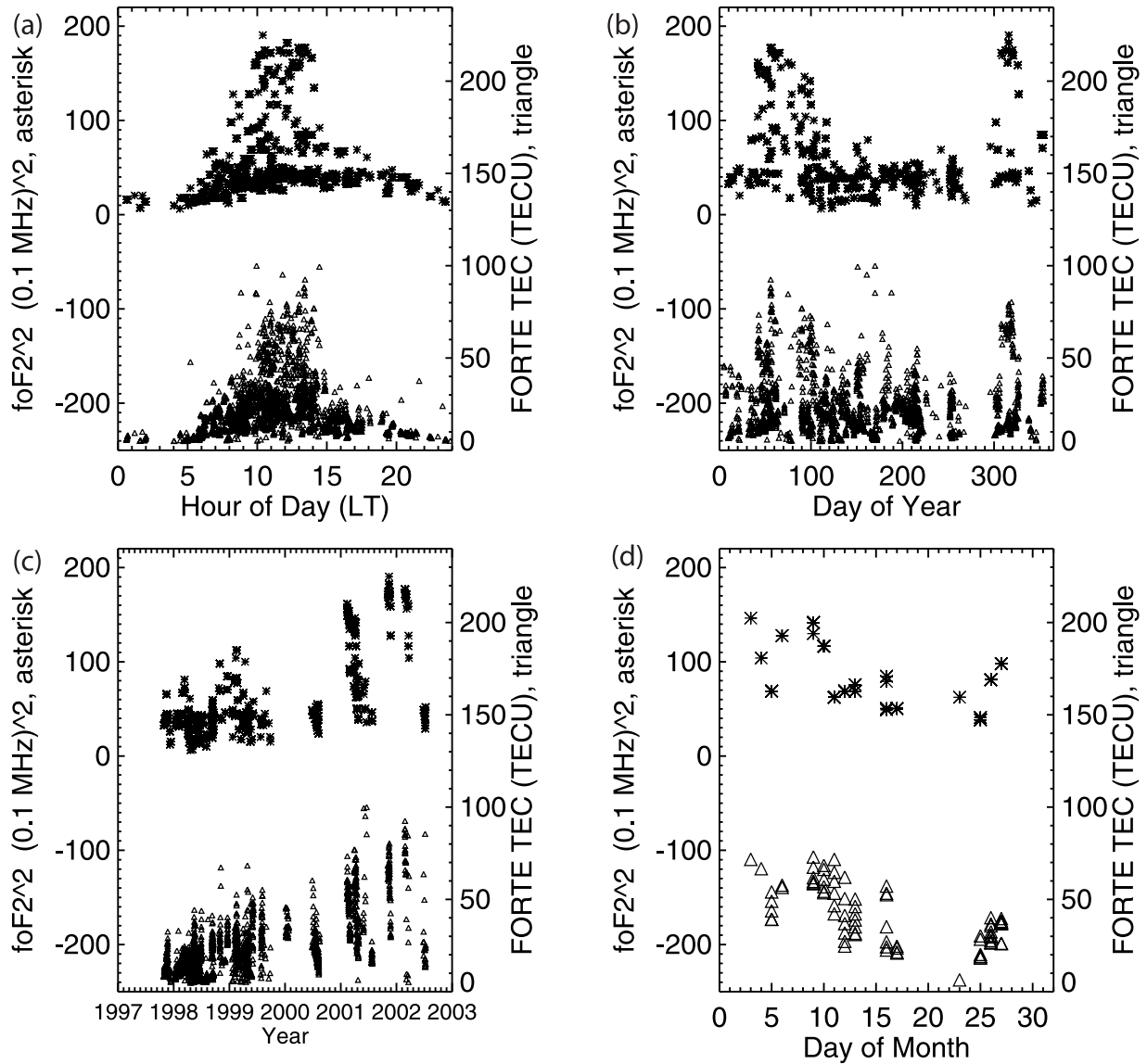


Figure 20. Comparisons of FORTE-derived TEC and ionosonde $(f_oF_2)^2$ for (a) diurnal variations, (b) seasonal variations, (c) interannual variations, and (d) 27-day solar cycle for 0800–1200 LT April 2001.

The correlation coefficients also show the differences in the relationship between TEC and f_oF_2 during low-high solar year, cold-warm season, and daytime-nighttime. For low solar activity year, TEC and f_oF_2 are better correlated during nighttime (close to 0.7) than during daytime (<0.5) no matter whether it is cold or warm season. For high solar activity year, the two are better correlated in warm season (>0.7) than in cold season (0.5) during daytime. This may indicate that the empirical linear fit function during low solar activity year nighttime or warm season daytime of high solar

Table 4. Correlation Coefficients for FORTE TEC and $(f_oF_2)^2$

	Day and Night	Day	Night
All Year	0.79	0.75	0.62
2001	0.56	0.35	0.55
1998	0.59	0.63	0.45
Jan–Apr	0.78	0.64	0.76
May–Aug	0.61	0.62	0.73
Sep–Dec	0.90	0.49	0.92
$K_p < 4o$	0.78	0.72	0.77
$K_p > 5o$	0.90	0.96	0.89

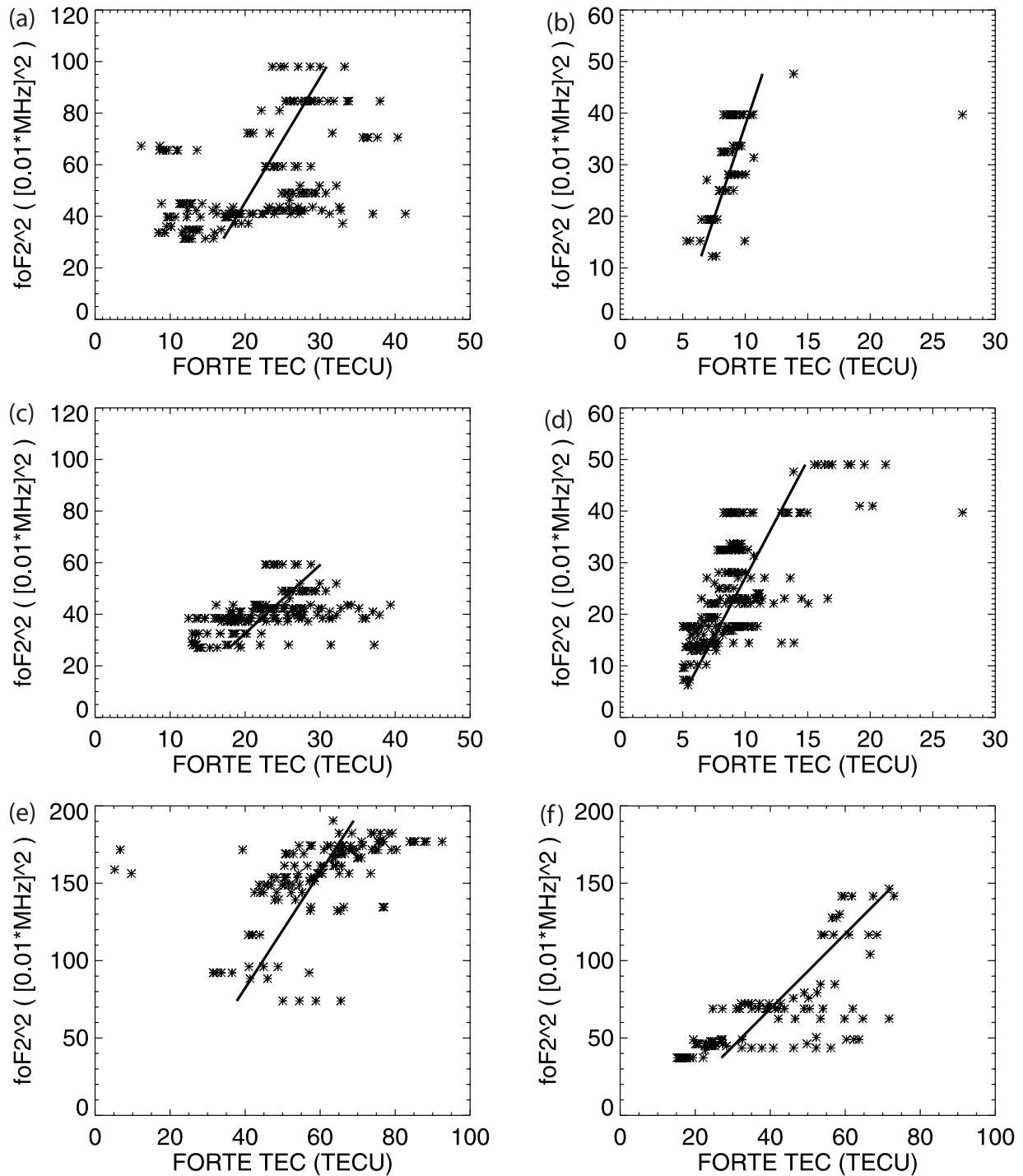


Figure 21. Relationship between FORTE-derived TEC and ionosonde critical frequency squared for (a) 1998 cold season daytime, (b) 1998 cold season nighttime, (c) 1998 warm season daytime, (d) 1998 warm season nighttime, (e) 2001 cold season, and (f) 2001 warm season.

Table 5. Linear Relationship Between FORTE TEC and Ionosonde (f_oF_2)² for Day-Night, Warm-Cold Season, and High-Low Solar Activity^a

	RMS	Percent RMS	Slope	Offset	Correlation Coefficient
1998 cold day	7.26	33.77	0.206	10.64	0.47
1998 warm day	5.46	23.98	0.377	7.705	0.46
1998 cold night	2.43	27.16	0.139	4.78	0.69
1998 warm night	3.33	35.32	0.219	4.08	0.68
2001 cold day	13.06	22.25	0.267	18.03	0.50
2001 warm day	11.53	29.67	0.412	11.64	0.73

$$^a\text{TEC} = \text{offset} + \text{slope} * (f_oF_2)^2.$$

activity year is probably close to the real relationship between TEC and f_oF_2 , while in other cases with correlation coefficients of smaller than 0.5, the fit functions are the most likely linear fit but the data are poorly correlated suggesting that the data are influenced by other external processes.

[50] Geomagnetic storms have significant effects on the magnitude of TEC and its transient fluctuations. It has been indicated that the increases in TEC have been observed at Los Alamos for most of the storm cases [Huang and Roussel-Dupré, 2005]. Table 6 shows the coefficients of the linear relationship between F_2 layer critical frequency and the TEC for different Kp index categories. It is interesting to note that for Kp index smaller than 5o the slope of the linear relationship is less variable, consistently in a range of 0.32–0.38, while showing a jump to 0.64 for Kp index greater than 5o that qualifies a geomagnetic storm.

[51] Our results show that the correlations between TEC and the F_2 region critical frequency are relatively high for geomagnetic disturbed conditions ($Kp > 5o$) when there observed a jump in the slope of the linear relationship between these two variables. A study by Liu *et al.* [2001] obtained a correlation coefficient of 0.953 between the GPS TEC and the f_oF_2 observed by the ionosonde at 25.0°N, 121.2°E for the 6 continuous days prior to the large earthquake ($M_w = 7.7$) occurred on 20 September 1999. If an earthquake may disturb the ionosphere as they suggested, i.e., “seismic” storms similar to geomagnetic storms, compared to 0.953 our correlation coefficients (0.89–0.96) for geomagnetically disturbed cases are consistent with Liu’s study.

5. Conclusions and Discussion

[52] The results from this comparative study suggest that the characteristics of the TEC variability at Los Alamos derived from various data sources are quantitatively in good agreement in terms of averaged TEC while display large differences when compared for transient events. For comparisons between the IRI model pre-

dicted and the FORTE-derived TECs, we found good agreements with RMS errors of smaller than 10.8% for annual or multiyear averaged comparisons while the differences are much larger with as large an RMS error as of 79.9% when compared for transient events during high solar activity years. For comparisons between ionosonde and FORTE data, we found percent RMS errors of about 22–43% when fitting transient TEC and the critical frequency into a linear relationship and a sharp increase in the slope of such relationship for Kp index greater than 5o. For comparisons between FORTE-derived TECs and local GPS TEC measurements on monthly means, we found good agreement for cold months with percent RMS errors of 4.6–6.2% and relatively poor agreement for warm months with percent RMS errors of 16.4–29.8%. Our analyses indicate that in predicting the TEC at Los Alamos, high solar activity years, summer time, and during geomagnetic storms are among the most likely to observe relatively large variations due to different types of data sources. Table 7 summarizes major characteristic differences found in our comparative study.

[53] Our study demonstrates that VHF broadband radio signal data can be used as a tool to validate ionospheric model predictions. The comparisons with the IRI model predicted TECs indicate areas in the IRI model that require special cautions in using the model outputs and improvements required for more reliable model predictions. The differences between the IRI model predictions and the FORTE-derived TECs when compared event specifically are particularly large at high solar activity years, suggesting that the IRI model-predicted TECs may not be reliable to describe the transient TECs at Los Alamos with reasonable RMS errors at high solar activity years. The areas that require improvements in the IRI model predictions also include over-predicted seasonal cycle and under-predicted 27-day solar cycle in daytime peak TEC amplitude.

[54] Our study also reveals the particular issues that should be taken into account for GPS TECs and for FORTE TECs. The FORTE-derived TECs agree better with the local GPS TEC measurements than the NOAA

Table 6. Linear Relationship Between FORTE TEC and Ionosonde (f_oF_2)² for Geomagnetic Storm Conditions^a

Kp Index	RMS	Percent RMS	Slope	Offset
<1o	9.496	39.71	0.331	4.174
1o–2o	10.83	39.99	0.324	7.185
2o–3o	10.31	43.25	0.360	5.219
3o–4o	10.33	35.27	0.347	8.006
4o–5o	7.971	32.05	0.385	4.648
>5o	9.836	32.86	0.639	–1.531

$$^a\text{TEC} = \text{offset} + \text{slope} * (f_oF_2)^2.$$

Table 7. Summary on the Differences Compared With FORTE TEC Variability

Differences Compared With FORTE TEC	
IRI-ITF model TEC	Event-specific differences are larger at high solar activity years than those at low solar activity years Model TEC is underpredicted in low TEC phase (May–Aug) and overpredicted in peak TEC phase (Jan–Apr)
NOAA GPS TEC	Model TEC is underpredicted on 27-day solar cycle GPS TEC is underpredicted for large TEC greater than 40 TECU GPS TEC is overpredicted for small TEC smaller than 10 TECU
AOA GPS TEC	GPS TEC decreases before noon instead of increases in the rising phase of diurnal cycle during summer months Variations in daytime GPS TEC from individual satellites are comparable to FORTE TEC day-to-day variations
Ionosonde critical frequency	Daytime correlations are higher in low solar activity years than in high solar activity years Linear relationships with $(f_oF_2)^2$ are largely seasonally, time of day, and storm effect–dependent

GPS TECs estimated using simple ionospheric mapping in terms of if the differences are biased. While simple ionospheric mapping works well for median TEC values, it may cause positive biases for very small TECs and negative biases for very large TECs. An issue needs to be addressed in deriving TEC from FORTE signals is the importance of the frequency-dependent quartic effects at the transionospheric VHF radio signals. Because of the much higher frequencies in GPS signals (1200–1500 MHz) than FORTE signals (30–100 MHz), GPS signals are much less or practically not subject to the quartic effects as the FORTE signals are. Preliminary experiments have been performed to the first-order TEC estimations using the upper portion and the lower portion of the spectrogram for a given FORTE signal and differences have been found in the derived slant TECs along the raypath. The best bandwidth of VHF broadband signals needs to be determined for better estimations of VHF TEC by comparing transient continuous overlapping GPS TEC measurements and VHF TEC measurements (to be discussed in a future paper).

[55] The results show us with directions for future studies using the FORTE-received LAPP signals. The larger FORTE TEC fluctuations compared with the IRI model predictions and the weaker correlations with the ionosonde F_2 region critical frequency during high solar activity years than those during low solar activity years are actually indicative of another type of TEC variability, which can be linked to ionospheric scintillation effects (to be studied in another paper). Furthermore, the relatively better correlations between the FORTE-derived TEC and the F_2 region critical frequency for geomagnetic storm conditions ($Kp > 5$) suggest that FORTE-derived TECs work better in storm conditions, which may be given more weight when combining various available TEC sources to characterize TEC during geomagnetic storm conditions, making the FORTE-derived TECs the more reliable source when ionospheric models are not valid during storm conditions.

[56] General descriptions of temporal variations of site ionospheric TEC at midlatitudes are necessary for scientific understanding as well as for practical applications such as communication and radar. However, efforts to improve the accuracy of transient TEC estimations and on the timescale for predicting TEC values in advance are important. An application of this comparative study would be possibly to develop a TEC prediction system for data fusion with a variety of input TEC data sources. Such a prediction system allows integration of many disparate types of data in the characterization of a time-dependent ionosphere providing improvement in temporal extrapolations for TEC predictions. The results from this study provide us a starting point to develop such a system with the evaluations of various TEC data sources in term of their quality and limitations under various conditions of solar activity and geomagnetic storm, for different seasons and time of day.

[57] **Acknowledgments.** This work was performed under the auspices of the United States Department of Energy. We are indebted to Phil Klingner and Abram Jacobson for support in acquiring and working with FORTE data and Robert Carlos for providing the GPS TEC measurement data from two AOA ICS-4000Z GPS receivers. We thank three anonymous reviewers for the depth of their analysis and commentary leading to the present version of this manuscript.

References

- Arikan, F., C. B. Erol, and O. Arikan (2003), Regularized estimation of vertical total electron content from Global Positioning System data, *J. Geophys. Res.*, *108*(A12), 1469, doi:10.1029/2002JA009605.
- Bilitza, D. (2001), International Reference Ionosphere 2000, *Radio Sci.*, *36*(2), 261–275.
- Breed, A. M., A.-M. Vandenberg, G. L. Goodwin, J. H. Silby, and E. A. Essex (1995), Measurement of the protonosphere in improving position determination using GPS satellites, in *Workshop on Applications of Radio Sci. (WARS 95) Digest*

- of *Papers*, edited by D. Skellern and J. Steel, pp. 3–6, Aust. Comm. for Radio Sci., Canberra.
- Brown, L. D., R. E. Daniel Jr., M. W. Fox, J. A. Klobuchar, and P. H. Doherty (1991), Evaluation of six ionospheric models as predictors of total electron content, *Radio Sci.*, 26(4), 1007–1015.
- Cander, L. R., J. Hickford, I. Tsagouri, and A. Belehaki (2004), Real-time dynamic system for monitoring ionospheric propagation conditions over Europe, *Electron. Lett.*, 40(4), 224–226.
- Codrescu, M. V., K. L. Beierle, T. J. Fuller-Rowell, S. E. Palo, and X. Zhang (2001), More total electron content climatology from TOPEX/Poseidon measurements, *Radio Sci.*, 36(2), 225–233.
- Conkright, R. O., K. Davies, and S. Musman (1997), Comparisons of ionospheric total electron contents made at Boulder, Colorado, using the Global Positioning System, *Radio Sci.*, 32(4), 1491–1497.
- Ephishov, I. I., L. W. Baran, I. I. Shagimutatorov, and G. A. Yakimoya (2000), Comparison of total electron content obtained from GPS with IRI, *Phys. Chem. Earth, Part C*, 25(4), 339–342, (Geosciences Research Division, GPS derived TEC: A TEC processing primer, National Geodetic Survey, NOAA, Silver Spring, Maryland, available at <http://www.ngs.noaa.gov/GRD/GPS/Projects/TEC/Library/TECprimer.html#MAPS>.)
- Ho, C. M., B. D. Wilson, A. J. Mannucci, U. J. Lindqwister, and D. N. Yuan (1997), A comparative study of ionospheric total electron content measurements using ionospheric maps of GPS, TOPEX radar, and the Bent model, *Radio Sci.*, 32(4), 1499–1512.
- Hoffmann-Wellenhof, B., H. Lichtenegger, and J. Collins (1997), *GPS: Theory and Practice*, Springer, New York.
- Huang, Z., and R. Roussel-Dupré (2005), Total electron content (TEC) variability at Los Alamos, New Mexico: A comparative study: FORTE-derived TEC analysis, *Radio Sci.*, 40, RS6007, doi:10.1029/2004RS003202.
- Jacobson, A. R., S. O. Knox, R. Franz, and D. C. Enemark (1999), FORTE observations of lightning radio-frequency signatures: Capabilities and basic results, *Radio Sci.*, 34(2), 337–354.
- Kersley, L., and J. A. Klobucher (1978), Comparison of protonospheric electron content measurements from the American and European sectors, *Geophys. Res. Lett.*, 5, 123–126.
- Lanyi, G. E., and T. Roth (1988), A comparison of mapped and measured total ionospheric electron content using Global Positioning System and beacon satellite observations, *Radio Sci.*, 23, 483–492.
- Lilensten, J., and L. R. Cander (2003), Calibration of the TEC derived from GPS measurements and from ionospheric models using the EISCAT radar, *J. Atmos. Sol. Terr. Phys.*, 65(7), 833–842.
- Liu, J. Y., Y. I. Chen, Y. J. Chuo, and H. F. Tsai (2001), Variations of ionospheric total electron content during the Chi-Chi earthquake, *Geophys. Res. Lett.*, 28, 1383–1386.
- Ma, G., and T. Maruyama (2002), A comparison of GPS-derived TEC and f_oF_2 over Japan, paper presented at 2002 General Assembly, Union Radio Sci. Int., Maastricht, Netherlands.
- Makela, J. J., S. A. Gonzales, B. MacPherson, X. Q. Pi, and M. C. Kelly (2000), Intercomparisons of total electron content measurements using the Arecibo incoherent scatter radar and GPS, *Geophys. Res. Lett.*, 27, 2841–2844.
- Mannucci, A. J., B. D. Wilson, and D. N. Yuan (1994), Monitoring ionospheric total electron content using the GPS global network and TOPEX/Poseidon altimeter data, in *Proceedings of the Beacon Satellite Symposium*, edited by L. Kersley, pp. 338–346, Univ. of Wales, Aberystwyth, U. K.
- Meza, A. M., C. A. Brunini, W. Bosch, and M. A. Vanzele (2002), Comparing vertical total electron content from GPS, Bent and IRI models with TOPEX-Poseidon, *Adv. Space Res.*, 30(2), 401–406.
- Paul, A. K. (1991), Applications for high-accuracy digital ionosonde data, *Radio Sci.*, 26(4), 949–958.
- Roussel-Dupré, R., A. R. Jacobson, and L. A. Triplett (2001), Analysis of FORTE data to extract ionospheric parameters, *Radio Sci.*, 36(6), 1615–1630.
- Sethi, N. K., V. K. Pandey, and K. K. Mahajan (2001), Comparative study of TEC with IRI model for solar minimum period at low latitude, *Adv. Space Res.*, 27(1), 45–48.
- Union Radio Scientifique Internationale (1993), *Handbook of Ionogram Interpretation and Reduction*, 2nd ed., WDC A, Rep. UAG-23, edited by W. R. Piggott and K. Rawer, Paris.
- Wilkinson, P., J. Wu, J. Du, and Y. J. Wang (2001), Real-time total electron content estimates using the International Reference Ionosphere, *Adv. Space Res.*, 27(1), 123–126.
- Wright, J. W. (1969), Some current developments in radio systems for sounding ionospheric structure and motions, *Proc. IEEE*, 57, 481–486.

Z. Huang and R. Roussel-Dupré, Atmospheric, Environmental and Climatic Dynamics Group, Earth and Environmental Sciences Division, Los Alamos National Laboratory, Los Alamos, NM 87545, USA. (zhen_huang@lanl.gov)